Cache Enabled UAV HetNets: Access - xHaul Coverage Analysis and Optimal Resource Partitioning

Neetu R.R, Gourab Ghatak, Anand Srivastava and Vivek Ashok Bohara

Abstract—We study an urban wireless network in which cache-enabled UAV-Access points (UAV-APs) and UAV-Base stations (UAV-BSs) are deployed to provide higher throughput and ad-hoc coverage to users on the ground. The cache-enabled UAV-APs route the user data to the core network via either terrestrial base stations (TBSs) or backhaul-enabled UAV-BSs through an xHaul link. First, we derive the association probabilities in the access and xHaul links. Interestingly, we show that to maximize the line-of-sight (LoS) unmanned aerial vehicle (UAV) association, densifying the UAV deployment may not be beneficial after a threshold. Then, we obtain the signal to interference noise ratio (SINR) coverage probability of the typical user in the access link and the tagged UAV-AP in the xHaul link, respectively. The SINR coverage analysis is employed to characterize the successful content delivery probability by jointly considering the probability of successful access and xHaul transmissions and successful cache-hit probability. We numerically optimize the distribution of frequency resources between the access and the xHaul links to maximize the successful content delivery to the users. For a given storage capacity at the UAVs, our study pre-scribes the network operator, the optimal bandwidth partitioning factors, and dimensioning rules concerning the deployment of the UAV-APs.

Index Terms—Cache-enabled UAVs, optimal resource allocation, success probability, 3D placement, xHaul.

I. INTRODUCTION

UNMANNED aerial vehicles (UAVs), mounted with remote radio heads (RRHs) can act as access points (either aerial relays or base stations (BSs)) to deliver reliable, cost-effective, and on-demand wireless connectivity to the ground users. They potentially enhance the coverage and capacity of cellular and ad-hoc networks. Such UAV networks have found applications in disaster relief scenarios, wireless sensor networks [1] and capacity augmentation in high-traffic areas [2]. The ability of the UAV-APs to adjust their 3D position in real-time can facilitate unobstructed line-of-sight (LoS) links to the ground users and maintain a reliable connection to the terrestrial base stations (TBSs) for the transport of the user data to the core network. Additionally, provisioning local storage at the UAV-APs by proactive caching can reduce the latency of the user applications while simultaneously reducing the load from the backhaul network. One of the most significant issues in the deployment planning of UAV-aided wireless networks is the design of backhaul links and its optimization with respect to user throughput by jointly taking into account the user density and the cache size. Based on the functionality available at the UAV-AP, specifically, the centralized and distributed units are split in the architecture [3], the link from the UAV-AP to a

The authors are with the Department of Electronics and Communication Engineering, IIT-Delhi, India. email: {neetur, gourab.ghatak, anand, vivek.b} @iiitd.ac.in.

UAV-BS or to a TBS can be classified as either a fronthaul or a midhaul. In this paper, we use the term *xHaul* to denote either of these types of links. The optimization of the access and xHaul is particularly challenging due to the temporally varying UAV and, user locations as well as the user requirements. In this regard, stochastic geometry provides an efficient tool to characterize the performance of UAV networks by assuming the locations of the UAVs and users as a spatial stochastic process and evaluating the key performance indicators (KPIs) in an expected sense. This equips the operator with essential dimensioning and initial deployment insights for such net-works. Consequently, in the proposed work, we develop a stochastic geometry model to jointly study the UAV access and xHaul links. Also, we investigate the optimal distribution of frequency resources between the access and xHaul network to maximize the content delivery success probability at the users by taking into account the storage capacity of the local cache at the UAV-APs.

A. Related Work

There has been an increasing interest in the use of UAVs as aerial BSs or relays, e.g., [4] - [6]. Integrating UAVs with legacy cellular networks results in vertical heterogeneous networks (HetNets) [7], which offer increased flexibility to the operator and enhanced coverage of the users. Additionally, provisioning of storage at the UAVs further augments the data rate and reduces the latency of services [8]. A comprehensive survey on UAV-assisted cellular communications can be found in the reference [9]. Contrary to TBSs, UAVs due to their controllable altitudes, can facilitate a higher probability of a direct LoS link to the users. In order to characterize the visibility conditions, authors in [10] have presented a tractable model that takes into account the height of buildings, the ratio of built-up area to total land area, and the number of buildings per unit area and have prescribed various visibility scenarios like suburban, urban, dense urban, and highrise urban. It may be noted that although the access link, i.e., UAV to user link, can be in a strong LoS state, the backhaul link, i.e., the UAV to the core network link, can potentially cause a bottleneck for high throughput or reliability-constrained applications. In this regard, integrated access and backhaul (IAB) is an attractive technology that efficiently exploits the same bandwidth to facilitate both access and backhaul connectivity [11]. The potentials and challenges of IAB for 5G mm-wave networks were investigated in [12]. The authors have highlighted the augmented throughput offered by IAB and the reduction in deployment costs. In our work, we investigate a scheme that partitions the bandwidth between the access and the backhaul

links and optimizes it for user throughput. Such a trade-off factor for resource allocation was studied in [13]. Furthermore, based on the achievable rate, they have formulated a resource allocation problem to enhance the user's data rate. However, they have not studied the impact of caching and the probability of successful content delivery at the user end. Additionally, from their work, the investigation of the impact of the intensity of UAVs on the association of user to the BSs for various visibility scenarios is missing, which can only be carried out either by extensive system-level simulations or using spatial stochastic processes.

The backhaul capacity impacts the placement of UAVs as well, which was investigated in [14], where the authors have proposed a backhaul-limited optimal UAV-BS placement algorithm and studied the effect of the user mobility on the UAV placement. Furthermore, the authors in [15] have investigated the trends in user-BS association with an increasing number of users for various caching schemes and corresponding bandwidth allocations while minimizing the total downlink transmit power. They also discussed the total backhaul capacity usage in aerial BSs while increasing the number of users in access links for different caching strategies. However, [15] does not explore the trade-offs in frequency resource partitioning between access and backhaul links. Specifically, in backhaul-constrained networks, proactive caching can improve the system performance by reducing the backhaul load. In [16], the authors have proposed a caching scheme by managing the content popularity to improve the success probability. They have analyzed the impact of the density of UAV-BSs, caching capacity, and the altitude of the UAVs on the successful content delivery, energy efficiency, and coverage probability of the network. The authors in [17] have formulated an optimization problem to minimize content delivery delay in UAV-non-orthogonal multiple-access networks. They have developed a reinforcement learning algorithm to investigate the effect of cache capacity, the number of cache contents, and the number of users on the content delivery delay. In this line of work, the authors in [18] have investigated the content distribution by offloading the traffic in hotspot areas by the combination of UAVs and edge caching. They have evaluated a mean opinion score (MOS) to obtain the quality of experience (QoE) of the users considering the user association, UAV placement and caching placement. Then a joint optimization problem is developed to maximize the MOS.

B. Motivation and Contribution

In [17] and [18], the authors have proposed efficient algorithms to optimize certain network parameters for a given realization of the network. However, using stochastic geometry-based analysis, we have given an expected view of the network by spatially averaging across all such network realizations. For example, the distribution of the efficacy of the proposed algorithms in [17] and [18] is challenging to derive, which may be possible using a stochastic geometry-based study. Also, in most of the prior works, the authors assume that the altitude of all the UAV access points to be the same and, consequently, optimize it with respect to the user metrics.

Motivated by this, we study a 3D spatial stochastic process to model the location of the UAVs. This is particularly challenging due to the requirement of distance distributions of UAVs restricted on a 3D half-plane. Additionally, the joint impact of caching and optimal distribution of frequency resources on user performance have not been studied in the existing research works. To investigate this, we propose a cache-enabled integrated access and x- haul (IAX) UAV wireless network overlaid on top of a legacy TBS network to sustain the QoS requirements of the ground users. The main contributions of this paper are summarized as follows:

1) We derive the distance distribution of (i) the nearest point on a 2-D plane from a typical point on a 3-D half-plane and (ii) the nearest point on a 3-D half-plane from a tagged point on the same 3-D half-plane, in a spherical representation of UAVs. Although the deployment of UAVs and their real-time locations span the 3D space, these spatial properties have previously not been reported in the literature on stochastic geometry-based models and are particularly challenging due to the non-isotropic nature of the spatial process in a 3D sense.

2) Leveraging these results, we derive the association probabilities of the typical user with the LoS/Non-line-of-sight (NLoS) UAV-APs and the TBSs for the access link. We explored the impact of densification of the network on the LoS link association. Furthermore, we derive the xHaul association probabilities of the tagged UAV-AP with either the UAV-BSs tier or the TBSs tier. A major challenge in such a characterization is the dependence of the xHaul link association probabilities on the access link association events. To the best of our knowledge, this paper is the first work that mathematically characterizes this dependence and derives complete access - xHaul association framework.

3) Based on the derived association probabilities, we obtain analytical expressions for the SINR coverage probability of the typical user associated to a LoS/NLoS UAVs or TBSs in the access link. Additionally, we derive the SINR coverage probability of the tagged UAV-AP associated to UAV-BS or TBS in the xHaul link by taking into account the statistical dependence of the access and the backhaul distances. The derived analytical expressions are then verified with extensive Monte-Carlo simulations.

4) In this network, we also study a caching scheme where the subset of the most popular contents are always stored locally at the UAV, while the remaining files are probabilistically cached. We analyze the impact of caching in the access-xHaul resource allocation. We optimize the resource partitioning factor between the access and xHaul for different cache sizes, the number of users, and the density of UAVs. We optimize the service success probability that jointly considers into account the end-to-end SINR coverage of the access link, the xHaul link, and the cache hit event. This reveals several key system designs and initial deployment insights to the network operator for deploying UAV-aided cellular networks.

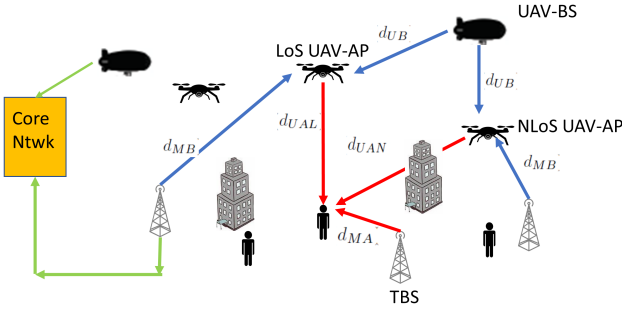The rest of the paper is organized as follows. In Section II we

Fig. 1. An illustration of the considered system model. The red and blue arrows are the access links and xHaul links, respectively. The green arrow is the wired/wireless link to the core network.

introduce our network model and outline the study objectives. Section III derives the relevant distance distributions and association probabilities. Based on this, in Sections IV and Section V, we derive the SINR coverage probability and the content delivery success probability, respectively. Then, in Section VI we validate our analytical framework and present some numerical results to discuss the salient features of the network. Finally, the paper concludes in Section VII.

II. SYSTEM MODEL

We consider a downlink heterogeneous network (HetNet) deployed for scenarios where the available wireless access infrastructure is insufficient, e.g., during mass events in areas not prepared for large crowds. The network consists of cache-enabled UAV-APs overlaid on top of a legacy TBSs consisting of macro base stations (MBSs) and small base stations (SBSs). The UAV-APs are small-sized low platform aerial vehicles, which connect to either the TBS or backhaul connected UAV-BS for xHaul support as given in Fig.1. The UAV-BSs are large-sized aerial vehicles with directional antennas for a good xHaul connection with the UAV-APs and core network. The users are assumed to be located co-planar with the TBS. The locations of the cached-enabled UAV-APs are modeled as a 3D poisson point process (PPP) Φ_U defined on $\mathbb{R}^2 \times \mathbb{R}^+$, with intensity λ_{UA}. On the contrary, the locations of the TBSs are modeled as a 2D PPP, Φ_M on $\mathbb{R}^2$, with intensity λ_M. Additionally, the locations of UAV-BSs are modeled as a 3D PPP Φ_B in $\mathbb{R}^2 \times \mathbb{R}^+$, with intensity λ_{UB}. Further, it is assumed that Φ_B is independent of Φ_U. Let $\Phi = \{X_l\}$ be the point process which is the union of all independent PPP in the network. Therefore, $\Phi = \Phi_M \cup \Phi_U \cup \Phi_B$. Without loss of generality, we perform the downlink analysis from the perspective of a typical user located at the origin of the 3D Euclidean space.

The typical user associates to either the UAV-AP tier or the TBS tier using Uu interface [19], based on the strongest BS association scheme in the access link. The received signal strength indicator (RSSI) measurements in the downlink access channel are estimated for the association of the typical user to the UAV-AP tier or the TBS tier. The association of the typical user to the UAV-BS is limited because of its high altitude. Given a UAV-AP association, in case the file requested by the user is present in the UAV cache, only the access link is used [20]. Otherwise, the UAV-AP retrieves the file from either the TBS tier or the UAV-BS tier via an xHaul link. In this work, we do not consider any local storage at the UAV-BS and the TBS tier due to the assumption of a reliable backhaul connection to the core network from these tiers. Thus, the UAV-AP associates with either the TBS tier or the UAV BS tier for xHaul transport using Xn interface [19], based on RSSI measurements. Restricting the heights of UAV-APs or UAV-BSs will not affect the association policy or further analysis. The UAV-BS increases the xHaul capacity by enabling additional wireless xHaul links. We assume UAV-APs and TBSs are equipped with downtilted omnidirectional antenna for access link and directional antennas for backhaul link [21]. As discussed before, the UAV-BSs are equipped with only directional antennas to provide backhaul support to the UAV-APs. Therefore, the association of the typical user to the UAV-BS is limited. We partition the total available bandwidth B between the access and the xHaul links using a bandwidth allocation factor, β which can take any value between 0 and 1, $\beta \in [0, 1]$ [22]. The allocated bandwidth to the access link is βB, and that to the xHaul link is $(1-\beta)B$ [13]. Moreover, we assume orthogonal frequency allocation to multiplex multiple users in the access link [23]. The downlink transmit powers of the UAV-APs, the backhaul connected UAV BSs, and the TBSs are P_{UA}, P_{UB}, and P_M, respectively.

A. Channel Model: Access link

The access link propagation consists of small-scale fading and large-scale path loss. Specifically, the TBSs transmissions experience small scale Rayleigh fading, g_M, with a variance of 1. The UAV-APs can either be in LoS or NLoS state from the perspective of the typical user. Let the locations of the UAV-APs in LoS and NLoS be denoted as Φ_L and Φ_N, respectively, where $\Phi_U = \Phi_L \cup \Phi_N$. The probability of LoS link between the UAV-AP and the typical user is given as [24]:

$$W_L(d, h) = \frac{1}{1 + \eta \exp\left(-\mu\left(\frac{180}{\pi}\sin^{-1}\left(\frac{h}{d}\right) - \eta\right)\right)} \quad (1)$$

where h is the height of the UAV-AP from the ground. The height h can be written in terms of the distance between the LoS UAV-AP and the typical user d, and θ which is the polar angle (angle between the polar axis and the line joining the typical user to the UAV-AP). Hence, $h = d\cos(\theta)$. Substituting in (1),

$$W_L(\theta) = \frac{1}{1 + \eta \exp\left(-\mu\left(\frac{180}{\pi}\sin^{-1}\left(\frac{d\cos(\theta)}{d}\right) - \eta\right)\right)} \quad (2)$$

Thus, $d\cos(\theta)$ is the height of the UAV-AP from the ground. From (1), it is evident that the probability of LoS transmission is independent of the distance d and only depends on θ and on the environment parameters. Here η and μ are the environment parameters for different visibility scenarios like suburban, urban, dense urban and high-rise urban. The η and μ values for different scenarios are suburban (4.88, 0.43), urban (9.61, 0.16), dense urban (11.95, 0.136), and high-rise urban (24.23, 0.08). Consequently, the probability of NLoS

$$A'_{MA} = \int_0^\infty \int_{C_{M1}}^\infty \left[\exp\left(-\frac{2}{3}\pi\lambda_{UA}W'_L\left(\left(\frac{P_{UA}}{P_M}\right)^{\frac{3}{\alpha_L}} w^{\frac{3\alpha_N}{\alpha_L}} \right) \right) - \exp\left(-\frac{2}{3}\pi\lambda_{UA}W'_L x^{\frac{3\alpha_N}{\alpha_L}} \right) \right] f_{d_{UAN}}(x)dx$$
$$\exp\left(-\frac{2}{3}\pi\lambda_{UA}W'_N\left(\left(\frac{P_{UA}}{P_M}\right)^{\frac{3}{\alpha_N}} w^{\frac{3\alpha_N}{\alpha_N}} \right) \right) f_{d_{MA}}(w)dw. \quad (3)$$

$$A''_{MA} = \int_0^\infty \int_{C_{M2}}^\infty \left[\exp\left(-\frac{2}{3}\pi\lambda_{UA}W'_N\left(\frac{P_{UA}}{P_M}\right)^{\frac{3}{\alpha_N}} w^{\frac{3\alpha_N}{\alpha_N}} \right) - \exp\left(-\frac{2}{3}\pi\lambda_{UA}W'_N x^{\frac{3\alpha_L}{\alpha_N}} \right) \right] f_{d_{UAL}}(x)d(x)$$
$$\exp\left(-\frac{2}{3}\pi\lambda_{UA}W'_L\left(\left(\frac{P_{UA}}{P_M}\right)^{\frac{3}{\alpha_L}} w^{\frac{3\alpha_N}{\alpha_L}} \right) \right) f_{d_{MA}}(w)dw. \quad (4)$$

$$A'_{UAL}(d_{UAL}) = \int_{C_{L1}}^\infty \left[\exp\left(-\frac{2}{3}\pi\lambda_{UA}W'_N d_{UAL}^{\frac{3\alpha_L}{\alpha_N}} \right) - \exp\left(-\frac{2}{3}\pi\lambda_{UA}W'_N\left(\frac{P_{UA}}{P_M}\right)^{\frac{3}{\alpha_N}} x^{\frac{3\alpha_N}{\alpha_N}} \right) \right]$$
$$\exp\left(-\pi\lambda_M\left(\frac{P_M}{P_{UA}}\right)^{\frac{2}{\alpha_N}} d_{UAL}^{\frac{2\alpha_L}{\alpha_N}} \right) f_{d_{MA}}(x)dx. \quad (5)$$

$$A''_{UAL}(d_{UAL}) = \int_{d_{UAL}^{\frac{\alpha_L}{\alpha_N}}}^\infty \left[\exp\left(-\pi\lambda_M\left(\frac{P_M}{P_{UA}}\right)^{\frac{2}{\alpha_N}} d_{UAL}^{\frac{2\alpha_L}{\alpha_N}} \right) - \exp\left(-\pi\lambda_M\left(\frac{P_M}{P_{UA}}\right)^{\frac{2}{\alpha_N}} x^{\frac{2\alpha_N}{\alpha_N}} \right) \right]$$
$$\exp\left(-\frac{2}{3}\pi\lambda_{UA}W'_N d_{UAL}^{\frac{3\alpha_L}{\alpha_N}} \right) f_{d_{UAN}}(x)dx. \quad (6)$$

transmissions are given as $W_N(\theta) = 1 - W_L(\theta)$. Due to the higher local scattering, the propagation model from an NLoS UAV to the typical user suffers from a Rayleigh fading g_{NL}. On the contrary, for the LoS UAV transmissions, we assume a Nakagami fading distribution, G_L, with shape parameter m. For the large scale path loss, we consider the classical power law where, the received power at the typical user from a TBS at a distance of d_{MA}, an LoS UAV at a distance of d_{UAL}, and an NLoS UAV at a distance of d_{UAN} is given by $R_{MA} = K_M P_M g_M(d_{MA})^{-\alpha_N}$, $R_{UAL} = K_U P_{UA} G_L(d_{UAL})^{-\alpha_L}$, and $R_{UAN} = K_U P_{UA} g_{NL}(d_{UAN})^{-\alpha_N}$, respectively. Here K_U and K_M are the path loss coefficients given by $K_U = K_M = (\frac{\lambda_c}{4\pi})^2$ where λ_c is the carrier wavelength. Whereas, α_L and α_N, are the path loss exponents.

B. Channel Model- xHaul link

We consider that because of the high altitude of UAV-APs compared to the TBSs, and the directional antennas in the UAV-BSs guarantee an LoS visibility state for the UAV-APs in the xHaul link [25], [26]. It must be noted that due to this assumption of LoS connectivity, the locations of the UAV-APs may be more accurately modeled by doubly stochastic point patterns. However, due to its independent scattering property, the PP model encapsulates the impact of multi-objective location optimization of the UAVs across realizations and allows us to derive macro-level system design and dimensioning rules. For a UAV-AP to UAV-BS xHaul link, we assume Nakagami distributed fast-fading, G_B, with parameter m [27]. On the contrary, the fast-fading for the xHaul link between a TBS and an UAV-AP suffers from a Rayleigh distributed fast-fading, g_B with variance equal to 1, since Rayleigh fading and Nakagami-m fading offer the same network performance in the strongest BS association scheme for a LoS transmission. [28]. Similar to the access link, we assume a power-law model for the large-scale path loss. Accordingly, the received power at a UAV-AP from a TBS located at a distance d_{MB} from it is

$R_{MB} = K_M P_M g_B(d_{MB})^{-\alpha_L}$, where, α_L is the path loss exponent. The received power at a UAV-AP from a backhaul connected UAV-BS is $R_{UB} = K_U P_{UB} G_B(d_{UB})^{-\alpha_L}$, where, α_L is the path loss exponent.

C. Caching Strategy

The UAV-APs are equipped with a local storage capability so as to provide rapid access of popular files to the users. The typical user randomly requests contents from the finite content database stored in UAV-AP, $\mathcal{J} = \{f_1, f_2, f_3, \ldots, f_L\}$, where the database size is L. We assume that each file has the same size, which is normalized to one. A subset of the database is locally cached at the UAV-APs. The popularity of the files is modeled according to the Zipf law [29]. In particular, the popularity or the content request probability of the ith file is given as: $a_i = \frac{i^{-\gamma}}{\sum_{j=1}^L j^{-\gamma}}$, where $\gamma \geq 0$ is the popularity factor. For $\gamma = 0$, all the files are of equal popularity i.e., $a_i = a_j$ $\forall$ $i > j$. For $\gamma > 0$, the trend of popularity of files follows a decreasing pattern, such as $a_i > a_j$ $\forall$ $i > j$. In fact, if $\gamma > 0$, the popularity of the files is given as i.e. $a_1 > a_2 > a_3 \ldots a_L$. The sum of content request probability is unity i.e., $\sum_{i=1}^L a_i = 1$. We assume that the UAV-APs can store up to C contents where $C \leq L$ [30]. We adopt a probabilistic caching strategy to store the files in the UAV-APs. The probability that the ith file is stored in the cache or its caching probability is denoted as b_i. Naturally, the caching probability satisfies the condition: $\sum_{i=1}^L b_i \leq C, 0 \leq b_i \leq 1, \forall i$. In our scheme, we split the cache size into two parts: the first part of the cache stores the most popular content (MPC) and the second part stores the less popular content (LPC). In particular, let us consider that there are C_0 MPC files. Accordingly, we cache all the MPC files, i.e., we set $b_i = 1$, $\forall 1 \leq i \leq C_0$. The remaining $C - C_0$ space of the cache is used to probabilistically

$$A'_{MA} = \frac{W'_L}{W'_L + W'_N} \int_0^\infty \exp\left(\frac{-2}{3}\pi\lambda_{UA}\left(W'_L + 2W'_N\right)w^3\right) f_{d_{MA}}(w)dw \tag{7}$$

$$A''_{MA} = \frac{W'_N}{W'_L + W'_N} \int_0^\infty \exp\left(\frac{-2}{3}\pi\lambda_{UA}\left(W'_N + 2W'_L\right)w^3\right) f_{d_{MA}}(w)dw \tag{8}$$

$$A'_{UAN}(d_{UAN}) = \int_{C_{N1}}^\infty \left[\exp\left(-\frac{2}{3}\pi\lambda_{UA}W'_L d_{UAN}^{\frac{3\alpha_N}{\alpha_L}}\right) - \exp\left(-\frac{2}{3}\pi\lambda_{UA}W'_L(\frac{P_{UA}}{P_M})^{\frac{3}{\alpha_L}}x^{\frac{3\alpha_N}{\alpha_L}}\right)\right]\exp\left(-\pi\lambda_M(C_{N1})^2\right)f_{d_{MA}}(x)dx. \tag{9}$$

$$A''_{UAN}(d_{UAN}) = \int_{d_{UAN}^{\frac{\alpha_N}{\alpha_L}}}^\infty \left[\exp\left(-\pi\lambda_M(N_2)^2\right) - \exp\left(-\pi\lambda_M(N_3)^2\right)\right]\exp\left(-\frac{2}{3}\pi\lambda_{UA}W'_L d_{UAN}^{\frac{3\alpha_N}{\alpha_L}}\right)f_{d_{UAL}}(x)dx. \tag{10}$$

$$\mathbb{P}\left(R_{UAL} > R_{UAN} > R_{MA}|\theta\right) = \int_{C_{L1}}^\infty \left[\exp\left(-2\pi\lambda_{UA}W'_N \int_0^{\left(\frac{h_L}{\cos(\theta)}\right)^{\frac{\alpha_L}{\alpha_N}}} z^2 dz\right) - \exp\left(-2\pi\lambda_{UA}W'_N \int_0^{L_1} y^2 dy\right)\right]$$
$$\exp\left(-\pi\lambda_M(C_{L1})^2\right)f_{d_{MA}}(x)dx, \tag{11}$$

$$\mathbb{P}\left(R_{UAL} > R_{MA} > R_{UAN}|\theta\right) = \int_{\left(\frac{h_L}{\cos(\theta)}\right)^{\frac{\alpha_L}{\alpha_N}}}^\infty \left[\exp\left(-\pi\lambda_M\left(L_2\right)^2\right) - \exp\left(-\pi\lambda_M\left(L_3\right)^2\right)\right]$$
$$\exp\left(-2\pi\lambda_{UA}W'_N \int_0^{\left(\frac{h_L}{\cos(\theta)}\right)^{\frac{\alpha_L}{\alpha_N}}} x^2 dx\right)f_{d_{UAN}}(x)dx, \tag{12}$$

cache the remaining $L - C_0$ files by setting:

$$b_i = \min\left(\frac{a_i(C - C_0)}{1 - \sum_{j=1}^{C_0} a_j}, 1\right) \quad \forall C_0 + 1 \le i \le C$$

Then, the cache hit probability at the UAV-AP, $\mathcal{P}_{hit}$ is defined as the probability that the requested content by a user is cached in the nearest UAV-AP [30]. This is discussed further in Section V. A successful content delivery at the user can occur in either of the following possibilities:

1) The user is associated to the TBS tier, and the user is under coverage from the nearest TBS. This event is denoted by S_t.
2) The user is associated to the UAV-AP tier, and:
   a) The requested file is cached at the nearest UAV-AP, and the user is under coverage from the nearest UAV-AP. In this case, the UAV-AP delivers the file without xHaul support. This event is denoted as S_a.
   b) The requested file is not cached at the nearest UAV-AP, however, the user is under coverage from it, and the UAV-AP is under coverage from either the nearest TBS or the nearest backhaul connected UAV BS via the xHaul link. This event is denoted as S_x.

The success probability P_{suc} is given as

$$P_{suc} = \mathbb{P}\left(S_t\right) + \mathbb{P}\left(S_a\right) + \mathbb{P}\left(S_x\right) \tag{13}$$

In this regard, the definition and the characterization of *coverage* is discussed in Section IV and the individual terms of the equation above are derived in Section V.

III. RELEVANT DISTANCE DISTRIBUTIONS AND ASSOCIATION PROBABILITIES

In this section, we derive the distance distributions of the potential access and the xHaul links. In what follows, based on the tier and the links, we use the subscript triplet ijk,

where $j \in \{A, B\}$ refers to either the access or backhaul and $i \in \{M, U\}$ refers to either the TBS or the UAV tier (UAV-AP in case $j = A$ and UAV-BS in case $j = B$). Furthermore, when $i = U$ and $j = A$, we have $k \in \{L, N\}$ representing the visibility state, i.e., LoS or NLoS. For all other i and j, we drop the subscript k for ease of notation.

First, let us note that the distance distribution of the typical user can be derived using the classical result of void probability of a PPP [31]:

Lemma 1. *The probability density function (pdf) of the distance between the typical user and closest TBS in the access link, d_{MA}, is given by $f_{d_{MA}}(x) = 2\pi\lambda_M x \exp\left(-\pi\lambda_M x^2\right)$.*

On the contrary, the UAV-APs can be categorized into having either an LoS or NLoS visibility state. The corresponding distance distributions are presented in the following lemma.

Lemma 2. *The pdf of the distances between the typical user and closest LoS and the closest NLoS UAV-AP, denoted by d_{UAL} and d_{UAN}, respectively, are given by*

$$f_{d_{UAL}}(x) = 2\pi\lambda_{UA}x^2 W'_L \exp\left(-\frac{2}{3}\pi\lambda_{UA}W'_L x^3\right), \tag{14}$$

$$f_{d_{UAN}}(x) = 2\pi\lambda_{UA}x^2 W'_N \exp\left(-\frac{2}{3}\pi\lambda_{UA}W'_N x^3\right), \tag{15}$$

where $W'_L = \int_{-\pi/2}^{\frac{\pi}{2}} W_L(\theta)\sin(\theta)d\theta$ and $W_L(\theta)$ is the probability of an LoS connection averaged over the polar angle, and $W'_N = \int_{-\pi/2}^{\frac{\pi}{2}} (1 - W_L(\theta))\sin(\theta)d\theta$.

The distance distribution between tagged UAV-AP at random height and UAV-BS, and between tagged UAV-AP and TBS in xHaul link is given in the next lemma.

Lemma 3. *The probability density function of distances between tagged UAV-AP and closest TBS on the ground, and between tagged UAV-AP and UAV-BS for xHaul, is denoted*

$$A_{UB}(d_a, \theta) = \int_{d_a \cos(\theta)}^{\ell(d_a, \theta)} 1 - \exp\left(-\frac{4}{3}\pi\lambda_{UB}\left(\frac{P_M}{P_{UB}}x^{-\alpha_L}\right)^{-\frac{3}{\alpha_L}}\right) f_{d_{MB}}(x)dx + \int_{\ell(d_a, \theta)}^{\infty} F''_{d_{UB}}\left(\left(\frac{P_M}{P_{UB}}d_{MB}^{-\alpha_L}\right)^{-\frac{1}{\alpha_L}}\right) f_{d_{MB}}(x)dx. \quad (16)$$

$$\mathcal{P}_{CM}(t_a) = \int_0^{\infty} \left(\exp\left(\frac{-t_a N_0}{K_M P_M q^{-\alpha_N}}\right) I'_{M1} I'_{L1} I'_{NL1}\right) f_{d_{MA}}(q)dq. \quad (17)$$

$$I'_{L1} = \exp\left(-2\pi\lambda_{UA}W'_L \int_{J_L}^{\infty}\left[x^2 dx - x^2\left(\frac{m}{m + \frac{\eta t_a K_U P_{UA} x^{-\alpha_L}}{K_M P_M q^{-\alpha_N}}}\right)^m dx\right]\right). \quad (18)$$

$$I'_{NL1} = \exp\left(-2\pi\lambda_{UA}W'_N \int_{J_{NL}}^{\infty}\left[y^2 dy - y^2\left(\frac{1}{1 + \frac{t_a K_U P_{UA} y^{-\alpha_N}}{K_M P_M q^{-\alpha_N}}}\right)dy\right]\right). \quad (19)$$

by $f_{d_{MB}}$ and $f_{d_{UB}}$ respectively, is given by (where $h = d\cos(\theta)$):

$$f_{d_{MB}}(x|d, \theta) = 2x\pi\lambda_M \exp\left(-\pi\lambda_M(x^2 - h^2)\right), \ x \geq h \quad (20)$$

$$f_{d_{UB}}(x|d, \theta) = \begin{cases} f'_{d_{UB}}(x), & x \leq h. \\ f''_{d_{UB}}(x|d, \theta), & x > h, \end{cases} \quad (21)$$

$$f'_{d_{UB}}(x) = 4\pi\lambda_{UB}x^2 \exp\left(-\lambda_{UB}\frac{4}{3}\pi x^3\right).$$

$$f''_{d_{UB}}(x|d, \theta) = 2\pi\lambda_{UB}\left(x^2 + xh\right) \\ \exp\left[-\lambda_{UB}\left(\frac{2}{3}\pi x^3 + x^2\pi h - \frac{1}{3}\pi h^3\right)\right],$$

where h is the height of the tagged UAV-AP from the ground. In case of LoS UAV-AP association, $h = d_{UAL}\cos(\theta)$ and for NLoS UAV-AP association, $h = d_{UAN}\cos(\theta)$. Here $\theta \sim \mathcal{U}\left[-\frac{\pi}{2}, \frac{\pi}{2}\right]$ is the uniformly distributed random orientation of the tagged UAV-AP from the typical user [32]. We use the variable d_a to jointly refer to either d_{UAL} or d_{UAN}.

Proof: See Appendix A. ∎

A. Access Link Association Probabilities

As discussed earlier, that in the access link, the typical user can either associate to a TBSs or an LoS/NLoS UAV-APs, based on the maximum power received at the user. For a typical user, the probability of getting associated to a TBS is presented in the following lemma.

Lemma 4. *The probability that the typical user is associated with the TBS in access link, A_{MA}, is given by:*

$$A_{MA} = A'_{MA} + A''_{MA}, \quad (22)$$

A'_{MA} and A''_{MA} are given in (3) and (4) where $C_{M1} = \left(\frac{P_{UA}}{P_M}\right)^{\frac{1}{\alpha_N}} w^{\frac{\alpha_N}{\alpha_N}}$, $C_{M2} = \left(\frac{P_{UA}}{P_M}\right)^{\frac{1}{\alpha_L}} w^{\frac{\alpha_N}{\alpha_L}}$,

Proof: The proof is presented in Appendix B. ∎

Solving with a special case: 1) $P_{UA} = P_M$ 2) $\alpha_N = \alpha_L$ where A'_{MA} and A''_{MA} are given in (7) and (8) respectively.

Note that we have averaged out on the distance distribution of the nearest TBS from the typical user. However, for a UAV-AP association, the association probabilities need to be derived conditioned on the respective access distances because of its impact on the backhaul association. The LoS and NLoS UAV-AP association in the access link is discussed next.

Lemma 5. *For a given d_{UAL}, the probability that the typical user is associated with the LoS UAV-AP in access link, is:*

$$A_{UAL}(d_{UAL}) = A'_{UAL}(d_{UAL}) + A''_{UAL}(d_{UAL}), \quad (23)$$

$$A'_{UAL}(d_{UAL}) = \mathbb{P}\left(R_{UAL} > R_{UAN} > R_{MA}|d_{UAL}\right).$$

$A'_{UAL}(d_{UAL})$ is given in (5) where $C_{L1} = \left(\frac{P_M}{P_{UA}}\right)^{\frac{1}{\alpha_N}} d_{UAL}^{\frac{\alpha_L}{\alpha_N}}$.

$$A''_{UAL}(d_{UAL}) = \mathbb{P}\left(R_{UAL} > R_{MA} > R_{UAN}|d_{UAL}\right).$$

$A''_{UAL}(d_{UAL})$ is given in (6)

Proof: The proof is same as Lemma 4 given in Appendix B. ∎

We note that the probability of LoS UAV-AP association in the access link, de-conditioned on d_{UAL} is given by:

$$\bar{A}_{UAL} = \int_0^{\infty} A_{UAL}(x)f_{d_{UAL}}(x)dx. \quad (24)$$

The above expression prescribes required deployment densities of the UAV-APs. Interestingly, in order to maximize the LoS UAV association, extreme densification can be detrimental as discussed below:

Proposition 1. *$\bar{A}_{UAL} \to 0$ as $\lambda_{UA} \to \infty$ and has at least one maxima with respect to λ_{UA}. Accordingly, there exists optimal UAV densities which maximizes the probability of association of typical user with the LoS UAV-AP.*

Proof. See Appendix C. □

Lemma 6. *For a given d_{UAN}, the probability that the typical user is associated with the NLoS UAV-AP in access link, is:*

$$A_{UAN} = A'_{UAN}(d_{UAN}) + A''_{UAN}(d_{UAN}). \quad (25)$$

$$A'_{UAN}(d_{UAN}) = \mathbb{P}\left(R_{UAN} > R_M > R_{UAL}\right).$$

$$A''_{UAN}(d_{UAN}) = \mathbb{P}\left(R_{UAN} > R_{UAL} > R_M\right).$$

$$I'_{L2} = \exp\left(-2\pi\lambda_{UA}W'_L\int_{J'_L}^{\infty}\left[y^2 dy - y^2\left(\frac{m}{m + \frac{\eta t_a y^{-\alpha_L}}{d_{UAN}^{-\alpha_N}}}\right)^m dy\right]\right), I'_{NL2} = \exp\left(-2\pi\lambda_{UA}W'_N\int_{d_{UAN}}^{\infty}\left(1 - \frac{1}{1 + \frac{t_a x^{-\alpha_N}}{d_{UAN}^{-\alpha_N}}}\right)x^2 dx\right). \quad (26)$$

$$I'_{M3} = \exp\left(-2\pi\lambda_M\int_{J''_M}^{\infty}\left[tdt - t\left(\frac{1}{1 + \frac{n\eta t_a K_M P_M t^{-\alpha_N}}{K_U P_{UA} d_{UAN}^{-\alpha_L}}}\right)dt\right]\right), I'_{L3} = \exp\left(-2\pi\lambda_{UA}W'_L\int_{d_{UAL}}^{\infty}\left[x^2 dx - x^2\left(\frac{m}{m + \frac{n\eta t_a x^{-\alpha_L}}{d_{UAL}^{-\alpha_L}}}\right)^m dx\right]\right). \quad (27)$$

$$I'_{NL3} = \exp\left(-2\pi\lambda_{UA}W'_N\int_{J''_{NL}}^{\infty}\left[y^2 dy - y^2\left(\frac{1}{1 + \frac{n\eta t_a y^{-\alpha_N}}{d_{UAL}^{-\alpha_L}}}\right)_m dy\right]\right). \quad (28)$$

$$I'_{U4} = \exp\left(-2\pi\lambda_{UB}W'_L\int_{J'_{BM}}^{\infty}\left[x^2 dx - x^2\left(\frac{m}{m + \frac{t_b K_U P_{UB} x^{-\alpha_L}}{K_M P_M d_{MB}^{-\alpha_L}}}\right)dx\right]\right). \quad (29)$$

$$I'_{M5} = \exp\left(-2\pi\lambda_M\int_{J'_{BU}}^{\infty}\left[tdt - t\left(\frac{1}{1 + \frac{n\eta t_b K_M P_M t^{-\alpha_L}}{K_U P_{UB} d_{UB}^{-\alpha_L}}}\right)dt\right]\right), I'_{U5} = \exp\left(-2\pi\lambda_{UB}W'_L\int_{d_{UB}}^{\infty}\left[x^2 dx - x^2\left(\frac{m}{m + \frac{n\eta t_b x^{-\alpha_L}}{d_{UB}^{-\alpha_L}}}\right)^m dx\right]\right). \quad (30)$$

$A'_{UAN}(d_{UAN})$ and $A''_{UAN}(d_{UAN})$ are given in (9) and (10) respectively, where $C_{N1} = \left(\frac{P_M}{P_{UA}}\right)^{\frac{1}{\alpha_N}} d_{UAN}^{\frac{\alpha_N}{\alpha_N}}$, $N_2 = \left(\frac{P_M}{P_{UA}}\right)^{\frac{1}{\alpha_N}} d_{UAN}^{\frac{\alpha_N}{\alpha_N}}$, $N_3 = \left(\frac{P_M}{P_{UA}}\right)^{\frac{1}{\alpha_N}} x^{\frac{\alpha_L}{\alpha_N}}$.

As a result, the probability of NLoS UAV-AP association in the access link, de-conditioned on d_{UAL} is given by: $\bar{A}_{UAN} = \int_0^{\infty} A_{UAN}(x)f_{d_{UAN}}(x)dx$. It can be verified with algebraic manipulations as well as numerically (as discussed in Section VI), that $A_{MA} + \bar{A}_{UAL} + \bar{A}_{UAN} = 1$.

Corollary 1. *When taking into account the height of UAV-APs, increasing the height of LoS UAV-AP will significantly decrease the association of typical user with the LoS UAV-AP.*

Proof. According to the RSSI based association scheme, the typical user connects to the LoS UAV-AP tier when either of the following events are true:

(i) $R_{UAL} > R_{UAN} > R_{MA}$ (ii) $R_{UAL} > R_{MA} > R_{UAN}$
The probability of event (i) can be written as

$$\mathbb{P}\left(P_{UA}d_{UAL}^{-\alpha_L} > P_{UA}d_{UAN}^{-\alpha_N} > P_M d_{MA}^{-\alpha_N}\right). \quad (31)$$

Representing the distance between user and LoS UAV-AP, d_{UAL} in terms of height of LoS UAV-AP, h_L and θ, i.e. $d_{UAL} = \frac{h_L}{\cos(\theta)}$. Here $\theta \sim \mathcal{U}\left[-\frac{\pi}{2}, \frac{\pi}{2}\right]$ is the uniformly distributed random orientation of the tagged UAV-AP from the typical user. Taking expectation over d_{MA} conditioning on θ, the final expression written as (11) and (12), where $C_{L1} = \left(\frac{P_M}{P_{UA}}\right)^{\frac{1}{\alpha_N}}\left(\frac{h_L}{\cos(\theta)}\right)^{\frac{\alpha_L}{\alpha_N}}$, $L_1 = \left(\frac{P_{UA}}{P_M}\right)^{\frac{1}{\alpha_N}} x^{\frac{\alpha_N}{\alpha_N}}$, $L_2 = \left(\frac{P_M}{P_{UA}}\right)^{\frac{1}{\alpha_N}}\left(\frac{h_L}{\cos(\theta)}\right)^{\frac{\alpha_L}{\alpha_N}}$, $L_3 = \left(\frac{P_M}{P_{UA}}\right)^{\frac{1}{\alpha_N}} x^{\frac{\alpha_N}{\alpha_N}}$. Adding (11) and (12), we get the probability of LoS UAV-AP association in the access link A_{UAL}, de-conditioned on θ is given by: $\bar{A}_{UAL}(h_L) = \int_{-\pi/2}^{\pi/2} A_{UAL}(\rho)f_\theta(\rho)d(\rho)$, where $f_\theta(\rho) = \frac{1}{\pi}$. So, as we increase the height of LoS UAV-AP h_L, the LoS association probability $\bar{A}_{UAL}$ decreases. This is because, as h_L increases, the received power from the LoS UAV-AP at the typical user decreases. Thus the probability of associating to NLoS UAV-AP/TBS increases.

Further, we can derive the probability of associating to NLoS UAV-AP, $\bar{A}_{UAN}$, by keeping the distance of LoS UAV-AP from the typical user in terms of h_L and θ. Furthermore, we can derive the probability of associating to TBS $\bar{A}_M$. $\square$

B. xHaul Link Association Probabilities

Next, we consider the xHaul link in case of a UAV-APs association in the access link. As discussed before, the xHaul association probabilities are dependent on the access link distance, d_a of the tagged UAV-AP from the typical user. Depending on the visibility state of the tagged UAV-AP from the typical user, the d_a can either be d_{UAL} or d_{UAN}. The tagged UAV-AP associates with either the TBS tier or a backhaul connected UAV-BS tier for xHaul support. Similar to the access link, the xHaul association is also based on RSSI measurements. The probabilities are given in the following lemma.

Lemma 7. *The probability, $A_{UB}(d_a, \theta)$ that the tagged UAV-AP associates to the UAV-BS tier for xHaul support is given in (16), where,*

$$\ell(d_a, \theta) = \left((d_a\cos(\theta))^{-\alpha_L}\frac{P_{UB}}{P_M}\right)^{-\frac{1}{\alpha_L}},$$

and $F''_{d_{UB}}(x)$ is the CDF corresponding to the pdf $f''_{d_{UB}}(\cdot)$ given in (21). The expansion of $F''_{d_{UB}}(x)$ is given in Appendix B.

Naturally, the probability that the tagged UAV-AP associates to the TBS tier for xHaul support is $A_{MB}(d_a, \theta) = 1 - A_{UB}(d_a, \theta)$.

Proof: See Appendix D. ∎

IV. CHARACTERIZATION OF SINR COVERAGE PROBABILITY

The SINR coverage probability for the typical user, $\mathcal{P}_C$ is defined as the probability that the received SINR Γ at the typical user is greater than a SINR threshold T, i.e.,

$$\mathbb{P}(S_a) = \mathcal{P}_{hit}\left(\underbrace{\left(\int_0^\infty A_{UAL}(x)\mathcal{P}_{CL}(x,t_a)f_{d_{UAL}}(x)dx\right.}_{I} + \underbrace{\int_0^\infty A_{UAN}(x)\mathcal{P}_{CN}(x,t_a)f_{d_{UAN}}(x)dx}_{II}\right) \tag{32}$$

$$\mathbb{P}(S_x) = \mathcal{P}_{miss}\left[\int_{-\frac{\pi}{2}}^{\frac{\pi}{2}}\left(\int_0^\infty (A_{UAL}(x)\mathcal{P}_{CL}(x,t_a)B_l(x,\theta))\,f_{d_{UAL}}(x)dxd\theta\right)+\right.$$
$$\left.\int_{-\frac{\pi}{2}}^{\frac{\pi}{2}}\left(\int_0^\infty A_{UAN}(x)\mathcal{P}_{CN}(x,t_a)B_l(x,\theta)f_{d_{UAN}}(x)dxd\theta\right)\right] \tag{33}$$

$$B_l(x,\theta) = \int_0^\infty A_{UB}(x,\theta)\mathcal{P}_{CUB}(y,t_b)f_{d_{UB}}(y|x,\theta)dy + \int_{x\cos(\theta)}^\infty A_{MB}(x,\theta)\mathcal{P}_{CMB}(x,t_b)f_{d_{MB}}(y|x,\theta)dy \tag{34}$$

$\mathcal{P}_C = \mathbb{P}(\Gamma > T)$. Ergodically, this represents the fraction of users that are under SINR coverage from the network. In the following, we adapt the same notation as above and denote the instantaneous SINR and the corresponding coverage probability by Γ_{ijk} and $\mathcal{P}_{ijk}$, respectively.

Lemma 8. *The SINR coverage probability of the typical user associated to the TBS in the access link is given in (17), where I'_{M1}, I'_{L1} and I'_{NL1} are the interference terms from other TBSs, LoS and NLoS-UAVs, respectively. t_a is the SINR threshold in the access link and $f_{d_{MA}}(q)$ is the pdf of the distances between user and closest TBS.*

$$I'_{M1} = \exp\left(-2\pi\lambda_M\int_{d_{MA}}^\infty\left(1 - \frac{1}{1+\frac{t_a t^{-\alpha_N}}{q^{-\alpha_N}}}\right)tdt\right). \tag{35}$$

I'_{L1} and I'_{NL1} are given in (18) and (19) respectively, where $J_L = \left(\frac{P_{UA}}{P_M}\right)^{\frac{1}{\alpha_L}}q^{\frac{\alpha_N}{\alpha_L}}$, $W'_L = \int_{-\pi/2}^{\frac{\pi}{2}}W_L(\theta)\sin(\theta)d\theta$ and $\eta = m(m!)^{\frac{-1}{m}}$, $J_{NL} = \left(\frac{P_{UA}}{P_M}\right)^{\frac{1}{\alpha_N}}q^{\frac{\alpha_N}{\alpha_N}}$, $W'_N = \int_{-\pi/2}^{\frac{\pi}{2}}(1 - W_L(\theta))\sin(\theta)d\theta$.

Lemma 9. *Given an NLoS and LoS UAV-AP association, the SINR coverage probability of the typical user in the access link is given respectively as:*
1) NLoS UAV-AP:

$$\mathcal{P}_{CN}(d_{UAN},t_a) = \exp\left(\frac{-t_a N_0}{K_U P_{UA}d_{UAN}^{-\alpha_N}}\right)\cdot I'_{M2}\cdot I'_{L2}\cdot I'_{NL2}. \tag{36}$$

I'_{NL2}, I'_{L2} and I'_{M2} are interference terms from other NLoS, LoS UAV-APs and TBSs respectively.

$$I'_{M2} = \exp\left(-2\pi\lambda_M\int_{J'_M}^\infty\left(1 - \frac{1}{1+\frac{t_a K_M P_M t^{-\alpha_N}}{K_U P_{UA}d_{UAN}^{-\alpha_N}}}\right)tdt\right),$$

I'_{L2} and I'_{NL2} are given in (26), where $J'_M = \frac{P_M}{P_{UA}}^{\frac{1}{\alpha_N}}d_{UAN}^{\frac{\alpha_N}{\alpha_N}}$ and $J'_L = d_{UAN}^{\frac{\alpha_N}{\alpha_L}}$.
2) LoS UAV-AP:

$$\mathcal{P}_{CL}(d_{UAL},t_a) = \sum_{n=1}^m (-1)^{n+1}\cdot{}^mC_n$$
$$\exp\left(\frac{-n\eta t_a N_0}{K_U P_{UA}d_{UAL}^{-\alpha_L}}\right)I'_{M3}I'_{L3}I'_{NL3}, \tag{37}$$

I'_{L3}, I'_{NL3} and I'_{M3} are interference terms from other LoS, NLoS UAV-APs and TBSs respectively. It is given in (27) and (28), where $J''_M = \frac{P_M}{P_{UA}}^{\frac{1}{\alpha_N}}d_{UAL}^{\frac{\alpha_L}{\alpha_N}}$ and $J''_{NL} = d_{UAL}^{\frac{\alpha_L}{\alpha_N}}$.

Proof: See Appendix E. ∎

Lemma 10. *The SINR coverage probability of the tagged UAV-AP associated to the TBS in the xHaul link is given as*

$$\mathcal{P}_{CMB}(d_{MB},t_b) = \exp\left(\frac{-t_b N_0}{K_M P_M (d_{MB})^{-\alpha_L}}\right)\cdot I'_{M4}\cdot I'_{U4}, \tag{38}$$

I'_{M4} and I'_{U4} are interference terms from other TBSs and UAV-BSs respectively. t_b is the SINR threshold in the xHaul link.

$$I'_{M4} = \exp\left(-2\pi\lambda_M\int_{d_{MB}}^\infty\left(1 - \frac{1}{1+\frac{t_b t^{-\alpha_L}}{(d_{MB})^{-\alpha_L}}}\right)tdt\right).$$

I'_{U4} is given in (29) where $J'_{BM} = \left(\frac{P_{UB}}{P_M}\right)^{\frac{1}{\alpha_L}}d_{MB}^{\frac{\alpha_L}{\alpha_L}}$.

Lemma 11. *The SINR coverage probability of the typical UAV-AP associated to the UAV-BS in the xHaul link is:*

$$\mathcal{P}_{CUB}(d_{UB},t_b) = \sum_{n=1}^m (-1)^{n+1}\cdot{}^mC_n$$
$$\exp\left(\frac{-n\eta t_b N_0}{K_U P_{UB}d_{UB}^{-\alpha_L}}\right)\cdot I'_{M5}I'_{U5} \tag{39}$$

I'_{U5} and I'_{M5} are interference terms from other UAV-BSs and TBSs respectively. The equations are given in (30) where $J'_{BU} = \frac{P_M}{P_{UB}}^{\frac{1}{\alpha_L}}d_{UB}^{\frac{\alpha_L}{\alpha_L}}$.

V. RATE COVERAGE AND CONTENT DELIVERY SUCCESS

The framework for SINR coverage probability can be employed to derive the rate coverage probability, which is defined as the probability that the per-user rate at the typical user is greater than a given threshold r_0. Mathematically, for N_u simultaneous users in the access link with orthogonal channel allocation, we have:

$$\mathbb{P}(R \ge r_0) = \mathbb{P}\left(\frac{\beta B}{N_u}\log_2(1+\Gamma) \ge r_0\right)$$
$$= \mathbb{P}\left(\Gamma \ge 2^{\frac{N_u r_0}{\beta B}} - 1\right) = \mathcal{P}_C\left(2^{\frac{N_u r_0}{\beta B}} - 1\right) \tag{40}$$

Let us assume that the minimum rate requirement in the access link to transfer a file requested by the user before the

service deadline be given by r_a. Accordingly, for a successful transmission, the access link SINR threshold is given by: $t_a = 2^{\frac{N_u r_a}{B\beta} - 1}$. Similarly, for an xHaul rate threshold of r_b, the xHaul SINR threshold: $t_b = 2^{\frac{r_b}{B(1-\beta)} - 1}$. Additionally, the cache hit probability or the probability that the requested the file is stored in the cache, $\mathcal{P}_{hit}$ is: $\mathcal{P}_{hit} = \sum_{i=1}^{C} a_i b_i$. Consequently, the probability that the requested file is not stored in the cache, $\mathcal{P}_{miss}$ is: $\mathcal{P}_{miss} = \sum_{i=1}^{C} a_i (1 - b_i)$. The successful content delivery of the user in (13) is defined as $\mathbb{P}(S_t) = A_{MA} \mathcal{P}_{CM}(t_a)$ and $\mathbb{P}(S_a)$ and $\mathbb{P}(S_x)$ are given in (32) and (33).

$B_l(x, \theta)$ in (34), is the total xHaul coverage probability. Here I is the SINR coverage probability of the user associated to LoS UAV-AP and II is the SINR coverage probability of the user associated to NLoS UAV-AP. Thus, we have characterized the different components of the expression (13) which characterize the content delivery success.

Solving with a special case: 1) $P_M = P_{UA} = P_{UB}$ 2) $\alpha_L = \alpha_N$ 3) $m = 1$
In Lemma 9, the SINR coverage probability of typical user in the access link for NLoS and LoS UAV-AP association is given as

$$\mathcal{P}_{CN}(d_{UAN}, t_a) = \left(\exp\left(\frac{-t_a N_0}{K_U P_{UA} d_{UAN}^{-\alpha_N}} \right) \cdot I'_{M2} \cdot I'_{L2} \cdot I'_{NL2} \right)$$

where $I'_{M2} \cdot I'_{L2} \cdot I'_{NL2}$ can be simplified as

$$I'_{M2} \cdot I'_{L2} \cdot I'_{NL2} = \exp\left(-2\pi \int_{d_{UAN}}^{\infty} \left[\left(1 - \frac{1}{1 + \frac{t_a t^{-\alpha_N}}{d_{UAN}^{-\alpha_N}}} \right) \right. \right.$$
$$\left. \left. \left(\lambda_M t + \lambda_{UA} W'_L t^2 + \lambda_{UA} W'_N t^2 \right) \right] dt \right)$$

Likewise, in Lemma 9, the SINR coverage probability of the typical user for LoS association is given as

$$\mathcal{P}_{CL}(d_{UAL}, t_a) = \sum_{n=1}^{m} (-1)^{n+1} \cdot {}^m C_n \exp\left(\frac{-n\eta t_a N_0}{K_U P_{UA} d_{UAL}^{-\alpha_L}} \right)$$
$$I'_{M3} I'_{L3} I'_{NL3},$$

where $I'_{M3} \cdot I'_{L3} \cdot I'_{NL3}$ is simplified as

$$I'_{M3} \cdot I'_{L3} \cdot I'_{NL3} = \exp\left(-2\pi \int_{d_{UAL}}^{\infty} \left[\left(1 - \frac{1}{1 + \frac{nt_a t^{-\alpha_N}}{d_{UAL}^{-\alpha_N}}} \right) \right. \right.$$
$$\left. \left. \left(\lambda_M t + \lambda_{UA} W'_L t^2 + \lambda_{UA} W'_N t^2 \right) \right] dt \right)$$

Similarly, in Lemma 10 and Lemma 11, the total interference power experienced when analyzing the SINR coverage probability of tagged UAV-AP to TBS and UAV-BS, respectively, is given as

$$I'_{M4} \cdot I'_{U4} = \exp\left(-2\pi \int_{d_{MB}}^{\infty} \left[\left(1 - \frac{1}{1 + \frac{t_b t^{-\alpha_N}}{d_{MB}^{-\alpha_N}}} \right) \right. \right.$$
$$\left. \left. \left(\lambda_M t + \lambda_{UB} W'_L t^2 \right) \right] dt \right)$$

$$I'_{M5} \cdot I'_{U5} = \exp\left(-2\pi \int_{d_{UB}}^{\infty} \left[\left(1 - \frac{1}{1 + \frac{nt_b t^{-\alpha_N}}{d_{UB}^{-\alpha_N}}} \right) \right. \right.$$
$$\left. \left. \left(\lambda_M t + \lambda_{UB} W'_L t^2 \right) \right] dt \right)$$

Consequently, the complexity of the rate coverage expression in (33) is reduced by three times, which significantly reduces the computation time.

VI. RESULTS AND DISCUSSIONS

In this section, we validate our analytical framework using Monte-Carlo simulations, providing a precise analysis equivalent to executing experiments, and present some numerical results to discuss the salient features of the network. The transmit powers are P_{UA}=27dBm [24], P_{UB}= 33 dBm [33] and P_M=46 dBm [23]. The thresholds are r_a= 1.1 Mbps [15] and r_b= 80 Mbps [14]. α_L=2, α_N=4, L=1000 [16] and B= 100 MHz [14].

We compare the performance gain or merits of the proposed framework in comparison with a benchmark work done in [34]. The authors in [34] have proposed an analytical model for any UE-UAV transceivers in terms of distributions of both UEs and UAVs without considering caching at the UAV end. They formulated a success probability of a ground-to-UAV transmission for a particular UE-UAV pair with zero caching ($C = 0$).

In Fig. 2, we plot the association probabilities of a typical user in the access link versus the intensity of UAV-AP for urban and high-rise urban scenarios. The environment parameters chosen for urban and high-rise urban are $a = 9.61$, $b = 0.61$ and $a = 24.23$, $b = 0.08$ respectively.

As discussed in Lemma 5, we note that the probability of LoS UAV-AP association increases with λ_{UA}, reaches a maximum, and decreases with further increase in λ_{UA}. This is because a fractional increase in the density increases the number of Los links for the very sparse deployment of UAVs. However, beyond a certain density, increasing the number of UAVs in the network further increases the potential of serving NLoS UAV-APs without substantially increasing the number of LoS links. We note that the intensity that maximizes the LoS UAV-AP association is lower for the urban environment than the urban high-rise environment due to larger blockage sizes. Intuitively, the TBS association decreases with an increasing number of UAVs in the network. Also, due to RSSI based association scheme, the access association probability does not depend on the intensity of users but only on the received powers from different tiers. Thus, this analysis equips the operator with an essential insight: in order to maximize LoS connectivity, densification of the network does not help beyond a certain limit. Accordingly, our analysis prescribes the optimal deployment density to maximize the LoS association for a given blockage environment.

In Fig. 3, we plot the association probabilities of a user in the access link versus the height of LoS UAV-AP. We observe that as the height of LoS UAV-AP increases, the LoS connection between the user and UAV-AP is interrupted, leading to a decrease in LoS UAV association probability. Moreover, as the
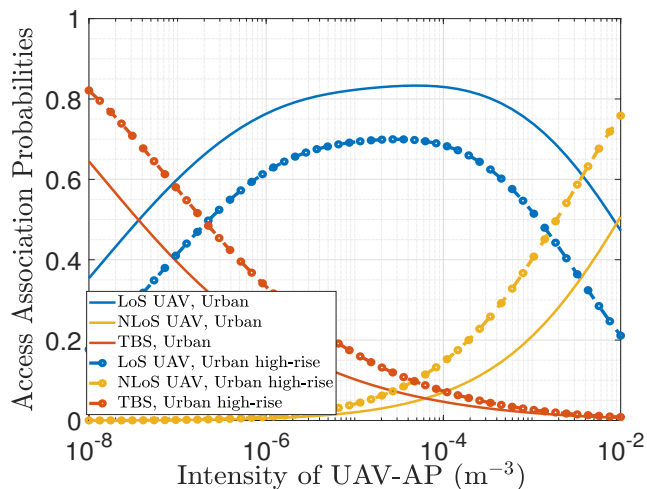
Fig. 2. Access association probabilities versus intensity of UAV-APs for the typical user in the access link for $\lambda_M = 10^{-6} m^{-2}$.
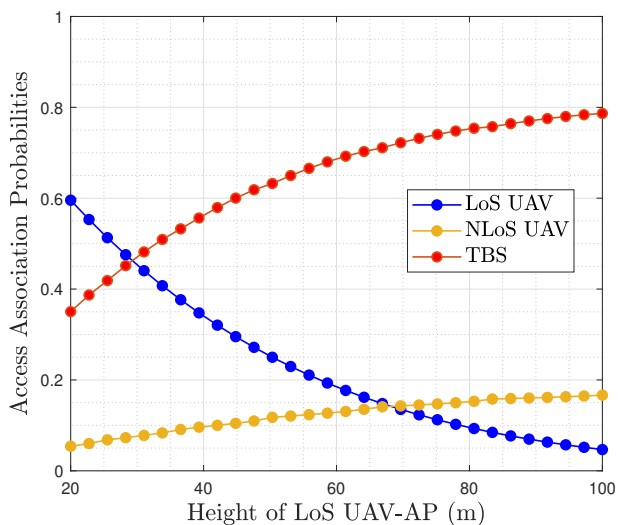

Fig. 3. Access association probabilities versus height of LoS UAV-AP

Fig. 4. xHaul association probabilities versus intensity of TBS for a typical UAV-AP in the xHaul link for $\lambda_{UA} = 10^{-5} m^{-3}$ and $\lambda_{UB} = 10^{-7} m^{-3}$.

Fig. 5. Overall coverage probability of the network versus SINR threshold for $\lambda_M = 10^{-6} m^{-2}$, $\lambda_{UA} = 10^{-5} m^{-3}$, $\eta = 9.61$, $\mu = 0.16$.

height of LoS UAV-AP increases, the association probability of TBS and NLoS UAV-AP increases. The association of TBS is more than NLoS UAV-AP due to limited blockages during the TBS transmission. We can obtain a height for LoS UAV-AP, for which the LoS UAV-AP association probabilities are the same as TBS association probabilities. At this height of UAV-AP, there is more than 45% chance for the user to associate to LoS UAV-AP or TBS and 10% chance to associate to NLoS UAV-AP to be under coverage. On the contrary, Fig. 4, shows that as the intensity of the TBSs tier increases, there is a monotonic increase and decrease of the TBS and UAV-BS association for xHaul support at a given UAV-AP.

Fig. 5 shows that the analytical result on the overall coverage probability closely matches the Monte-Carlo simulations. We validate the framework for different λ_{UA} values. Fig. 6 shows the probability of successful content delivery for a different number of simultaneously served users and cache sizes. Naturally, an increase in the cache size or a decrease in the number of users improves the per-user success probability.
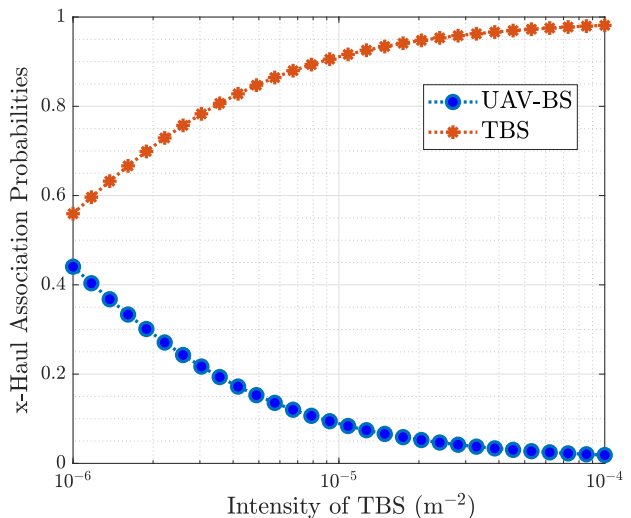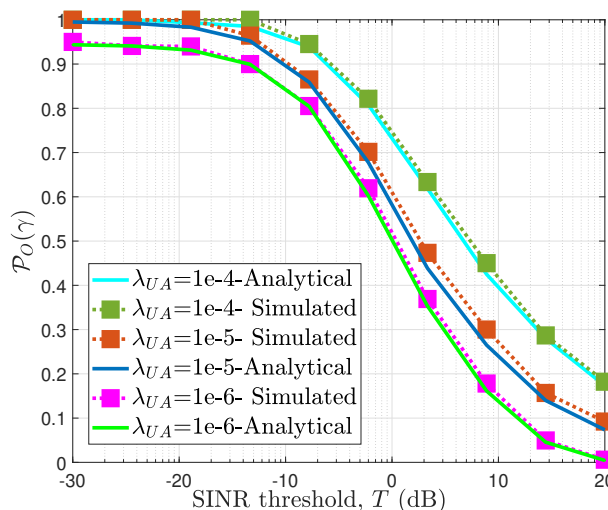
For the network operator, this reveals how our framework can be used to determine the number of simultaneously served users from one UAV-AP. For example, with $\lambda_{UA} = 10^{-5} m^{-3}$, with a cache size of $C = 600$, the typical user observes about 80% success if 5 users are served simultaneously. At the same time, it drops to about 50% if 8 users are served simultaneously. In case the operator wants to sustain success of over 90%, the operator must necessarily facilitate admission control mechanisms so that no more than 5 users are served simultaneously. This is because with 5 users, even caching all the files in the local storage does not achieve a success probability greater than 0.9.

In Fig. 7, we plot success probability versus the number of users in the access link by considering the benchmark scheme i.e., the cache size is zero. Naturally, as the number of users increases, the success probability in the network decreases. For cache size, $C=0$, gives the lowest success probability as

the requirement in the access link increases, and C=1000 gives the highest success probability. If the requirement in the access link is increased by three times, the success probability will decrease only by 22% if we cache more than 400 files at the UAV-AP locally. If the files are not cached, the success probability is decreased by 35%. Although, in general the success probability increases with an increase in the number of UAV-APs, extreme densification can be detrimental due to increased interference.

In Fig. 8 we plot the success probability with respect to λ_{UA} for different cache sizes and a fixed resource partitioning factor $\beta = 0.5$. As a dimensioning rule, this prescribes the network operator with deployment densities given the storage capacity of the local cache of the UAV-APs. For example, when the UAV-APs do not cache any file locally, like in the benchmark scheme i.e., $C = 0$, a success probability of beyond 0.9 is obtained only beyond $\lambda_{UA} = 0.01$ m^{-3}, On the contrary, with higher local storage, e.g., $C = 1000$, a success probability of 0.9 is achieved with 10 times fewer UAV-APs, i.e., $\lambda_{UA} = 0.001$ m^{-3}. In both cases, however, the success probability falls rapidly after $\lambda_{UA} = 0.5$ m^{-3} due to an increase in interference with densification. This effectively reduces the SINR and rate coverage probability. Recall from Fig. 2 that this region corresponds to a higher NLoS association, while all the LoS UAV-APs contribute to the interference. Until now, we discussed the results with an equal partitioning of frequency resources between the access and the x-hual link. Next, we study the impact of resource partitioning on the success probability.

Fig. 9 shows the success probability with respect to the resource partitioning factor β for different values of cache sizes for the urban scenario. Indeed, $C = 0$ refers to the case when all the files requested by the user from the UAV-AP is retrieved from the backhaul connected UAV-BS, which in our work is the benchmark scheme. In this case, $\beta = 1$, i.e., when all the resources are allotted to the access link, results in a 0% success although the access link achieves a high rate coverage. We note the existence of an optimum value of β, which maximizes the success probability. When some of the files are stored at the local cache (e.g., $C = 400, 800$, etc.), the operator may provide all the resources to the access link (thereby reducing the xHaul load) without degrading the success probability. In contrast, when all the files are stored in the local cache $C = 1000$, all the frequency resources must necessarily be allotted to the access link. The optimal β thus increases with increasing cache size. The optimal β trend with its corresponding optimal success probability is discussed next.

In Fig. 10, we plot optimal success probability versus cache size for different visibility scenarios. As cache size increases, the probability of successful delivery of contents to the user increases. For the suburban scenario, where the success probability is high due to less blockages, for C=1000, the success in content delivery is 100% i.e., all the users are delivered with the requested contents directly by the access link. On the contrary, for urban, urban high-rise and dense-urban scenarios, even caching all the files locally at the UAV-APs result in lower success.

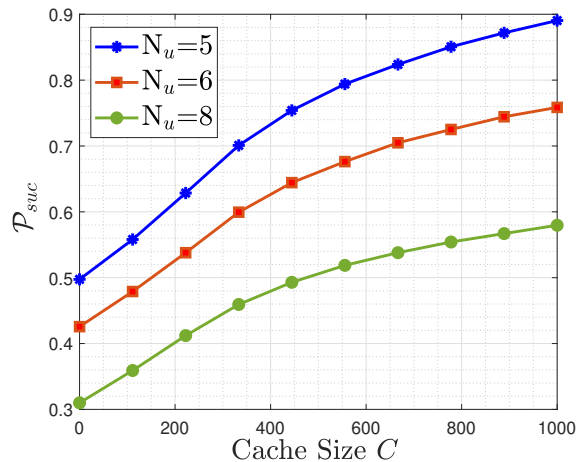In Fig. 11, we plot optimal β and success probability versus

Fig. 6. Success probability versus cache size for different values of N_u with $\lambda_M = 10^{-6} m^{-2}$, $\lambda_{UA} = 10^{-5} m^{-3}$, $\eta = 9.61$, $\mu = 0.16$.
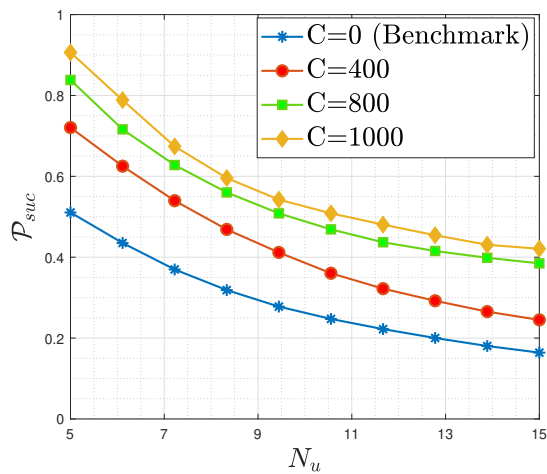

Fig. 7. Success Probability versus Number of users in the access link

cache size C for urban scenario. As the cache size increases, optimal β, along with the maximum success probability increases. In particular, let us consider two cases: $\gamma = 1$ and $\gamma = 0$. For $\gamma = 1$, i.e., when the files are of decreasing popularity, and the MPC are cached, the xHaul link is rarely accessed as compared to the case with $\gamma = 0$. Indeed, for $\gamma = 0$, for a given file request from the typical user, a $(1-C)/1000$ fraction of the time the xHaul support is needed to deliver the file. Accordingly, we observe a higher value of optimal β, i.e., more resources allocated to the access link for $\gamma = 1$ as compared to $\gamma = 0$. Similarly, due to a more frequent xHaul requirement, the success probability for the case with $\gamma = 0$ is lower as compared to $\gamma = 1$. This reveals that based on the popularity profile of the content, the network operator not only needs to design an optimal access - xHaul split, but also provision minimum local storage at the UAV-APs. For content popularity modeled with $\gamma = 1$, a cache size of $C = 700$ guarantees 84% success of content delivery. On the contrary, for equiprobable file popularity, storing 70% of the files in the local cache results in a limited ($< 75\%$) success. In such cases, the operator needs to re-dimension the network with either an increased deployment of
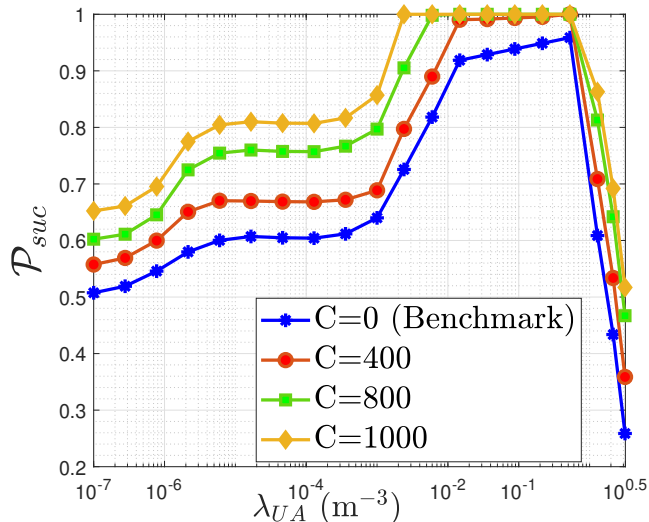
Fig. 8. Success probability versus intensity of UAV-AP for different values of C for $\lambda_M = 10^{-6}m^{-2}$.
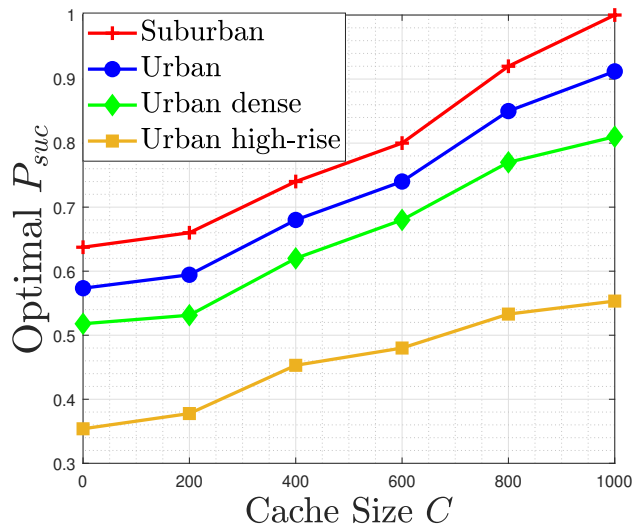

Fig. 10. Variation of optimal P_{suc} with respect to C for different visibility scenarios
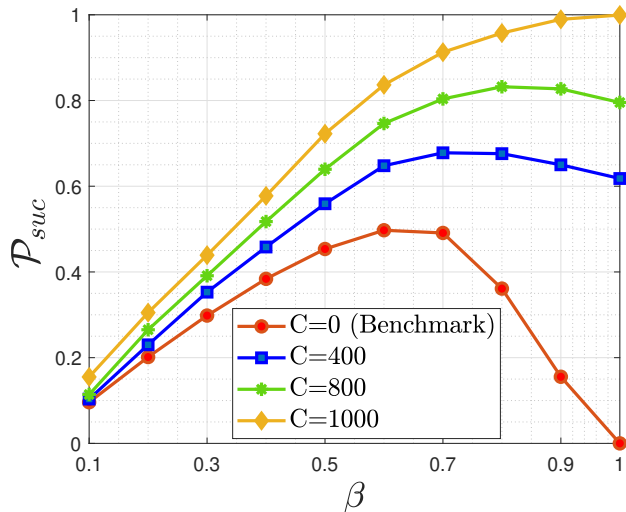

Fig. 9. Success probability versus the resource partitioning factor for different values of C for $C_0=C/2$.
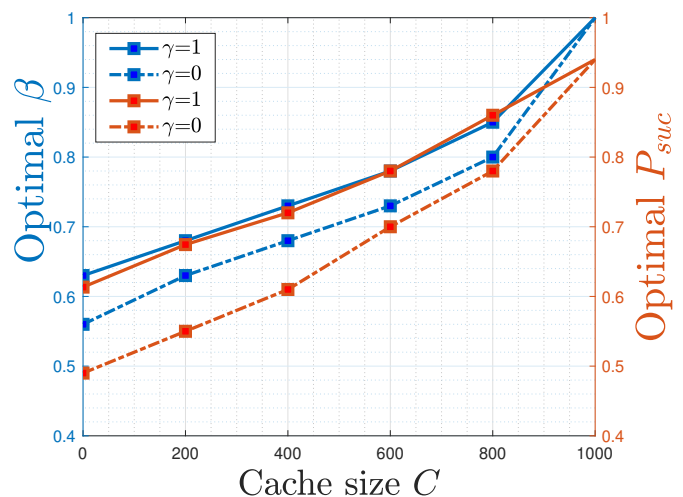

Fig. 11. Variation of optimal β and optimal P_{suc} with respect to C for different values of γ.

UAV-APs or provisioning advanced interference management mechanisms. However, when all the files are stored in the cache, $C = 1000$, the optimal probability of success is the same irrespective of the values of γ. For $\gamma = 1$, when the files are of decreasing popularity, and the MPC files are stored with a probability of one, more bandwidth is given to the access than xHaul. For $\gamma = 0$, when the files are of equal popularity, the probability of requesting the files stored in the cache will be less. Therefore, for the successful delivery of files to the user, xHaul is accessed. Thus, the optimal value of β is more for $\gamma = 1$ compared to $\gamma = 0$. Also, for $\gamma = 1$, the success probability is more when compared to $\gamma = 0$, except when all the files are stored in the cache.

VII. CONCLUSION

In UAV networks, the consideration of the xHaul link capacity and its joint optimization with the access link re-

quirement is imperative. In this work, we derived a joint framework for association and coverage analysis of the access and xHaul links in a UAV-aided cellular network. We showed that for maximizing the LoS association probability, network densification with deploying more UAVs beyond a threshold density does not help, and it deteriorates user performance. Accordingly, we prescribe optimal deployment densities to maximize LoS coverage probability. The distribution of frequency resources among the access and the xHaul link depends on the size of local storage size at the UAV-APs. Larger cache sizes result in a larger allocation of resources in the access link since the xHaul link is used less frequently as compared to smaller cache sizes. We also prescribed admission control strategies in terms of maximum simultaneously served users to sustain a per-user throughput above a threshold. The optimal resource split also depends on relative popularity of the files: the more equi-probable the file popularity is, the

$$F_{d_{UAL}}\left(d_{UAN}^{\frac{\alpha_N}{\alpha_L}}\right) - F_{d_{UAL}}\left(C_M d_{MA}^{\frac{\alpha_N}{\alpha_L}}\right) = \exp\left(-2\pi\lambda_{UA}W_L'\int_0^{\left(C_M d_{MA}^{\frac{\alpha_N}{\alpha_L}}\right)} z^2 dz\right) - \exp\left(-2\pi\lambda_{UA}W_L'\int_0^{\left(d_{UAN}^{\frac{\alpha_N}{\alpha_L}}\right)} y^2 dy\right) \quad (41)$$

$$\mathbb{P}\left(d_{UAN}^{\frac{\alpha_N}{\alpha_L}} > C_M d_{MA}^{\frac{\alpha_N}{\alpha_L}}\right) = \mathbb{E}_{d_{MA}}\left[\exp\left[-2\pi\lambda_{UA}W_N'\int_0^{C_M^{\frac{\alpha_L}{\alpha_N}} d_M^{\frac{\alpha_N}{\alpha_N}}} x^2 dx\right]\right] \quad (42)$$

$$A_{MA}' = \int_0^\infty \int_{C_{M1}}^\infty \left[\exp\left(-\frac{2}{3}\pi\lambda_{UA}W_L'\left(\left(\frac{P_{UA}}{P_M}\right)^{\frac{3}{\alpha_L}} w^{\frac{3\alpha_N}{\alpha_L}}\right)\right) - \exp\left(-\frac{2}{3}\pi\lambda_{UA}W_L' x^{\frac{3\alpha_N}{\alpha_L}}\right)\right]$$
$$f_{d_{UAN}}(x)dx \exp\left(-\frac{2}{3}\pi\lambda_{UA}W_N'\left(\left(\frac{P_{UA}}{P_M}\right)^{\frac{3}{\alpha_N}} w^{\frac{3\alpha_N}{\alpha_N}}\right)\right) f_{d_{MA}}(w)dw. \quad (43)$$

$$\underbrace{\int_0^\infty \int_{C_{L1}}^\infty \exp\left(-2\pi\lambda_{UA}W_N'\int_0^{d_{UAL}^{\frac{\alpha_L}{\alpha_N}}} z^2 dz\right)\exp\left(-\pi\lambda_M(C_{L1})^2\right)f_{d_{MA}}(x)f_{d_{UAL}}(y)dxdy}_{I} -$$
$$\underbrace{\int_0^\infty \int_{C_{L1}}^\infty \exp\left(-2\pi\lambda_{UA}W_N'\int_0^{L_1} y^2 dy\right)\exp\left(-\pi\lambda_M(C_{L1})^2\right)f_{d_{MA}}(x)f_{d_{UAL}}(y)dxdy}_{II} \quad (44)$$

larger should be the amount of resources allotted to the xHaul link, especially for small cache sizes. The consideration of mobility of the users and handover between different tiers are interesting directions of research that we will address in future work. Also, we will explore different association strategies, other than RSSI-based association scheme, which take performance metrics like throughput directly into account. We will study distributed caching and its impact on system performance and resource partitioning in the future.

VIII. ACKNOWLEDGEMENT

APPENDIX A
PROOF OF LEMMA 3

The CDF of d_{MB} is evaluated as:

$$F_{d_{MB}}(x) = 1 - \exp\left(-\pi\lambda_M\left(x^2 - h^2\right)\right) \quad (45)$$

where h is the height of the typical UAV-AP from the ground. Taking the derivation of (45), we can obtain $f_{d_{MB}}(x)$. The distance between the UAV-BS and UAV-AP is t. For $t \leq h$,

$$F_{d_{UB}}'(x) = 1 - \exp\left(-\lambda_{UB}\frac{4}{3}\pi x^3\right) \quad (46)$$

Taking the derivative of (46), $f_{d_{UB}}'(x|h)$ is obtained.

For $t > h$, the volume of the segment is given as

$$V_{t-h} = \frac{1}{3}\pi\left(t - h\right)^2\left(3t - (t - h)\right) = \frac{1}{3}\pi\left[2t^3 - 3t^2h + h^3\right]$$

The distance distribution is derived by considering the volume of the sphere from which the volume of the segment V_{t-h} is omitted.

$$F_{d_{UB}}''(x) = 1 - \exp\left[-\lambda_{UB}\left(\frac{2}{3}\pi x^3 + x^2\pi h - \frac{1}{3}\pi h^3\right)\right] \quad (47)$$

Taking the derivative of (47), we obtain $f_{d_{UB}}''(x|h)$.

APPENDIX B
PROOF OF LEMMA 4

The typical user associates to the TBS tier when either of the following events are true: Comparing the received powers from all TBS, LoS UAV-AP and NLoS UAV-AP.

(i) $R_{MA} > R_{UAL} > R_{UAN}$ (ii) $R_{MA} > R_{UAN} > R_{UAL}$ The probability of event (i) can be written as $\mathbb{P}\left(P_M d_{MA}^{-\alpha_N} > P_{UA}d_{UAL}^{-\alpha_L} > P_{UA}d_{UAN}^{-\alpha_N}|d_{UAL}\right)$.

Using the cdf of d_{UAL} from **Lemma 2**, for given instances of d_{UAN} and d_{MA}, the above equation can be written as:

$$\left[F_{d_{UAL}}\left(d_{UAN}^{\frac{\alpha_N}{\alpha_L}}\right) - F_{d_{UAL}}\left(C_M d_{MA}^{\frac{\alpha_N}{\alpha_L}}\right)|d_{UAN}, d_{MA}\right].$$
$$\mathbb{P}\left(d_{UAN}^{\frac{\alpha_N}{\alpha_L}} > C_M d_{MA}^{\frac{\alpha_N}{\alpha_L}}\right) \quad (48)$$

Considering the cdf terms separately, gives (41) and (42).

Taking the expectation with respect to d_{MA} and d_{UAN} over (41), and combine (41) and (42), gives (43), where $C_{M1} = \left(\frac{P_{UA}}{P_M}\right)^{\frac{1}{\alpha_N}} w^{\frac{\alpha_N}{\alpha_N}}$. Similarly, we can evaluate the probability of event (ii) to obtain A_{MA}'', where in the first step, we use the CDF of the variable d_{UAN}, and then take the expectation with respect to d_{MA} and d_{UAL}. Finally, adding A_{MA}' and A_{MA}'', we can obtain the probability of associating to TBS tier, A_{MA}. Solving with a special case, we obtain (7) and (8).

APPENDIX C
PROOF OF PROPOSITION 1

Recall the probability of LoS association in access link $\bar{A}_{UAL}$ is divided into two parts as:

$$\bar{A}_{UAL} = \int_0^\infty A_{UAL}'(d_{UAL})f_{d_{UAL}}(x)dx +$$
$$\int_0^\infty A_{UAL}''(d_{UAL})f_{d_{UAL}}(x)dx \quad (49)$$

The first part $\int_0^\infty A_{UAL}'(d_{UAL})f_{d_{UAL}}(x)dx$ can be written as in (44). In (44), $C_{L1} = \left(\frac{P_M}{P_{UA}}\right)^{\frac{1}{\alpha_N}} d_{UAL}^{\frac{\alpha_L}{\alpha_N}}$, $L_1 =$

$$\frac{d}{d\lambda_{UA}}\left[\int_0^\infty \int_{C_{L1}}^\infty \exp\left(-\frac{2}{3}\pi\lambda_{UA}W_N' y^{\frac{3\alpha_L}{\alpha_N}}\right)\exp\left(-\pi\lambda_M\left[\left(\frac{P_M}{P_{UA}}\right)^{\frac{2}{\alpha_N}} y^{\frac{2\alpha_L}{\alpha_N}}\right]\right)\right.$$

$$\left. \cdot 2\pi\lambda_M x \exp\left(-\pi\lambda_M x^2\right)2\pi\lambda_{UA}W_L' y^2 \exp\left(-\frac{2}{3}\pi\lambda_{UA}W_L' y^3\right)dxdy\right] \quad (50)$$

$$\frac{d}{d\lambda_{UA}}\left[\int_0^\infty 2\pi\lambda_{UA}y^2 W_L' \exp\left(-2\pi\lambda_M\left[\left(\frac{P_M}{P_{UA}}\right)^{\frac{2}{\alpha_N}} y^{\frac{2\alpha_L}{\alpha_N}}\right]\right)\exp\left(-\frac{2}{3}\pi\lambda_{UA}\left(W_N' y^{\frac{3\alpha_L}{\alpha_N}} + W_L' y^3\right)\right)dy\right] \quad (51)$$

$$\int_0^\infty \left[-\frac{4}{3}\pi\lambda_{UA}\left(W_N' y^{\frac{3\alpha_L}{\alpha_N}} + W_L' y^3\right)y^2 W_L' \exp\left(-2\pi\lambda_M\left[\left(\frac{P_M}{P_{UA}}\right)^{\frac{2}{\alpha_N}} y^{\frac{2\alpha_L}{\alpha_N}}\right]\right)\right.$$

$$\exp\left(-\frac{2}{3}\pi\lambda_{UA}\left(W_N' y^{\frac{3\alpha_L}{\alpha_N}} + W_L' y^3\right)\right) + 2\pi y^2 W_L' \exp\left(-2\pi\lambda_M\left[\left(\frac{P_M}{P_{UA}}\right)^{\frac{2}{\alpha_N}} y^{\frac{2\alpha_L}{\alpha_N}}\right]\right)$$

$$\left. \exp\left(-\frac{2}{3}\pi\lambda_{UA}\left(W_N' y^{\frac{3\alpha_L}{\alpha_N}} + W_L' y^3\right)\right)\right] \quad (52)$$

$$A_{UB}(d_a,\theta) = \int_{d_a\cos(\theta)}^{\ell(d_a,\theta)} 1 - \exp\left(-\frac{4}{3}\pi\lambda_{UB}\left(\frac{P_M}{P_{UB}}x^{-\alpha_L}\right)^{-\frac{3}{\alpha_L}}\right)f_{d_{MB}}(x)dx + \int_{\ell(d_a,\theta)}^\infty F_{d_{UB}}''\left(\left(\frac{P_M}{P_{UB}}d_{MB}^{-\alpha_L}\right)^{-\frac{1}{\alpha_L}}\right)f_{d_{MB}}(x)dx \quad (53)$$

$\left(\frac{P_{UA}}{P_M}\right)^{\frac{1}{\alpha_N}} d_{MA}^{\frac{\alpha_N}{\alpha_N}}$. To prove that there exists at least one maxima of the association probability with respect to λ_{UA}, let us observe the derivative of the first term of (44) that constitutes A_{UAL}' is given in (50). Applying Leibniz Integral rule in (51), gives (52).

At $\lambda_{UA} = 0$, (52) becomes

$$\int_0^\infty 2\pi y^2 W_L' \exp\left(-2\pi\lambda_M\left[\left(\frac{P_M}{P_{UA}}\right)^{\frac{2}{\alpha_N}} y^{\frac{2\alpha_L}{\alpha_N}}\right]\right)dy \quad (54)$$

which gives a positive value when substituting the values and integrate with respect to y. On the other hand, the derivative of II of (44) constitutes A_{UAL}'. Therefore, the derivative of A_{UAL}' is when λ_{UA} is zero. Similarly, we can prove the derivative of $\int_0^\infty A_{UAL}''(d_{UAL})f_{d_{UAL}}(x)dx$ in (49), with respect to λ_{UA} is also a positive function when $\lambda_{UA} = 0$. Thus, at $\lambda_{UA} = 0$, $\bar{A}_{UAL}$ is an increasing function of λ_{UA}. On the contrary, substituting $\lambda_{UA} = \infty$ directly in the expansion of (49), we note that both evaluate to zero. Consequently, there exists at least one maxima of $\bar{A}_{UAL}$ with respect to λ_{UA}, as $\bar{A}_{UAL}$ is an increasing function for $\lambda_{UA}=0$, and $\bar{A}_{UAL}$ is zero when $\lambda_{UA}= \infty$. Therefore, we can say that, there exists optimal UAV densities which maximizes the probability of association of typical user with the LoS UAV-AP.

APPENDIX D
PROOF OF LEMMA 7

Given an access link distance of d_a, the UAV-AP associates to a UAV-BS in case the received power from it is larger than the one received from a TBS. This probability is evaluated as:

$$A_{UB}(d_a,\theta) = \mathbb{P}\left(d_{UB} \leq \left(\frac{P_M}{P_{UB}}d_{MB}^{-\alpha_L}\right)^{-\frac{1}{\alpha_L}}\bigg| d_a\right) =$$

$$\mathbb{E}_{d_{MB}}\left[\mathcal{T}(d_{MB})\right]$$

$$\mathcal{T}(d_{MB}) = \begin{cases} 1 - \exp\left(-\frac{4}{3}\pi\lambda_{UB}\left(\frac{P_M}{P_{UB}}d_{MB}^{-\alpha_L}\right)^{-\frac{3}{\alpha_L}}\right); \\ \qquad d_{MB} \leq \left((d_a\cos(\theta))^{-\alpha_L}\frac{P_{UB}}{P_M}\right)^{-\frac{1}{\alpha_L}} \\ F_{d_{UB}}''\left(\left(\frac{P_M}{P_{UB}}d_{MB}^{-\alpha_L}\right)^{-\frac{1}{\alpha_L}}\right); \\ \qquad d_{MB} > \left((d_a\cos(\theta))^{-\alpha_L}\frac{P_{UB}}{P_M}\right)^{-\frac{1}{\alpha_L}} \end{cases}$$

The expectation is taken with respect to $f_{d_{MB}}$, which is defined only for $x \geq h$. Considering, $\ell(d_a,\theta) = \left((d_a\cos(\theta))^{-\alpha_L}\frac{P_{UB}}{P_M}\right)^{-\frac{1}{\alpha_L}}$, we note that for $P_{UB} \leq P_M$, we have $\left(\frac{P_{UB}}{P_M}\right)^{-\frac{1}{\alpha_L}} \geq 1$ and accordingly, $\left((d_a\cos(\theta))^{-\alpha_L}\frac{P_{UB}}{P_M}\right)^{-\frac{1}{\alpha_L}} \geq d_a\cos(\theta)$. Accordingly, the expectation with respect to d_{MB} evaluates to (53).

APPENDIX E
PROOF OF LEMMA 8

Given that the typical user has associated to TBS, the SINR coverage probability is given as

$$\mathcal{P}_{CM} = \mathbb{P}\left[\frac{K_M P_M d_{MA}^{-\alpha_N} g_M}{N_0 + I_{M1} + I_{L1} + I_{NL1}} > t_a\right] \quad (55)$$

where I_{M1}, I_{L1} and I_{NL1} are the interference strength from the tier of TBSs, LoS UAV-APs and NLoS UAV-BSs respectively, where $I_{M1} = \sum_{l:X_l\in\Phi_M'} K_M P_M d_{M,l}'^{-\alpha_N} \bar{g}_l'$, $I_{L1} = \sum_{l:X_l\in\Phi_L} K_U P_{UA} d_{L,l}^{-\alpha_L} \bar{G}_l$ and $I_{NL1} = \sum_{l:X_l\in\Phi_N} K_U P_{UA} d_{N,l}^{-\alpha_N} \hat{g}_l$. Φ_M' is the tier of TBSs in which the associated TBS is omitted. d_M' is the distance of user from the TBSs other than the associated TBS. d_L is the distance of user from the interfering LoS UAV-APs. d_N is the distance of user from the interfering NLoS UAV-APs. $\bar{g}$, $\bar{G}$ and $\hat{g}$ are the fast-fading coefficients from the interfering TBSs, LoS UAV-APs and NLoS UAV-APs respectively. Taking the expectation over the individually independent

TBS, LoS/NLoS UAV-AP tiers in (55), the interference terms are expressed as,

$$I'_{M1} = \mathbb{E}_{\Phi'_M}\left[\prod_{l:X_l\in\Phi'_M} \frac{1}{1+\frac{t_a d'^{-\alpha_N}_{M,l}}{d^{-\alpha_N}_{MA}}}\right]$$

Computing the moment generating function of exponential random variable $\bar{g}$, (35) is obtained.

$$I'_{L1} = \mathbb{E}_{\Phi_L}\left[\prod_{l:X_l\in\Phi_L} \left(\frac{m}{m+\frac{\eta t_a K_U P_{UA} d^{-\alpha_L}_{L,l}}{K_M P_M d^{-\alpha_N}_{MA}}}\right)^m\right] \quad (56)$$

where $\eta = m(m!)^{\frac{-1}{m}}$. Noting that $|\bar{G}|^2$ is a normalized gamma random variable with parameter m. Computing moment generating function of gamma random variable $\bar{G}$, we can obtain (18).

$$I'_{NL1} = \mathbb{E}_{\Phi_N}\left[\prod_{l:X_l\in\Phi_N} \frac{1}{1+\frac{t_a K_U P_{UA} d^{-\alpha_N}_{N,l}}{K_M P_M d^{-\alpha_N}_{MA}}}\right]$$

Solving these equations and substituting in (17), we can obtain $\mathcal{P}_{CM}$.

Similarly, the SINR coverage probability of typical user associated to LoS UAV is given as

$$\mathcal{P}_{CL} = \mathbb{P}\left[\frac{K_U P_{UA} d^{-\alpha_L}_{UAL} G_L}{N_0 + I_{M3} + I_{L3} + I_{NL3}} > t_a\right] \quad (57)$$

where I_{M3}, I_{L3} and I_{NL3} are the interference strength from the tier of TBSs, LoS UAV-APs and NLoS UAV-BSs respectively, where $I_{M3} = \sum_{l:X_l\in\Phi_M} K_M P_M d^{-\alpha_N}_{M,l} \bar{g}_l$, $I_{L3} = \sum_{l:X_l\in\Phi'_L} K_U P_{UA} d'^{-\alpha_L}_{L,l} \bar{G}'_l$ and $I_{NL3} = \sum_{l:X_l\in\Phi_N} K_U P_{UA} d'^{-\alpha_N}_{N,l} \hat{g}_l$. Φ'_L is the tier of LoS UAV-APs in which the associated LoS UAV-AP is omitted. d'_L is the distance of user from the LoS UAV-APs other than the associated LoS UAV-AP. $\bar{G}'$ is the fast-fading coefficient from the interfering LoS UAV-APs other than the associated LoS UAV-AP.

(57) can be written as $1 - \mathbb{E}_\Phi\left[\left(1-\exp\left(\frac{-\eta t_a(N_0+I_{M3}+I_{NL3}+I_{L3})}{K_U P_{UA} d^{-\alpha_L}_{UAL}}\right)\right)^m\right]$ where Φ is the union of the individual independent PPP. $\Phi = \Phi_M \cup \Phi'_L \cup \Phi_N$.

The above equation can be solved by Binomial theorem, applying expectation over the tiers and computing the moment generating function of gamma random variable $\bar{G}$, we can obtain (27) as derived before.

Solving these equations and substituting in (37), we can obtain P_{CL}. Similarly, we can obtain the SINR coverage probability of typical user associated to NLoS UAV, $\mathcal{P}_{CN}$ given in (36). The proof of SINR coverage probability of tagged UAV-AP associated to TBS or UAV-BS in the xHaul link follows in a similar way as Proof of Lemma 8.

References

[1] M. Hua, Y. Wang, Z. Zhang, C. Li, Y. Huang, and L. Yang, "Power-efficient communication in UAV-aided wireless sensor networks," *IEEE Communications Letters 22.6*, pp. 1264–1267, Apr 2018.

[2] P. Ji, X. Jia, Y. Lu, H. Hu, and Y. Ouyang, "Multi-UAV assisted multi-tier millimeter-wave cellular networks for hotspots with 2-Tier and 4-Tier network association," *IEEE Access 8*, pp. 158 972–158 995, Aug 2020.

[3] D. Harutyunyan and R. Riggio, "Flex5G: Flexible functional split in 5G networks," *IEEE Transactions on Network and Service Management*, vol. 15, no. 3, pp. 961–975, 2018.

[4] Xiao, Zhenyu, and et al., "A survey on millimeter-wave beamforming enabled uav communications and networking," *IEEE Communications Surveys & Tutorials 24.1 (2021)*, pp. 557–610, 11 2021.

[5] L. Zhang, A. Celik, S. Dang, and B. Shihada, "Energy-efficient trajectory optimization for uav-assisted iot networks," *IEEE Transactions on Mobile Computing (2021)*, Apr 2021.

[6] Cai, Yuanxin, and et al., "Resource allocation and 3D trajectory design for power-efficient IRS-assisted UAV-NOMA communications," *IEEE Transactions on Wireless Communications (2022)*, Jun 2022.

[7] Su, Zhou, and et al, "Uav enabled content distribution for internet of connected vehicles in 5g heterogeneous networks," *IEEE Transactions on Intelligent Transportation Systems, 22(8)*, pp. 5091–102, 08 2021.

[8] F. Cheng, G. Gui, N. Zhao, Y. Chen, J. Tang, and H. Sari, "UAV-relaying-assisted secure transmission with caching," *IEEE Transactions on Communications*, vol. 67, pp. 3140–3153, 5 2019.

[9] A. Fotouhi, H. Qiang, M. Ding, M. Hassan, L. G. Giordano, A. Garcia-Rodriguez, and J. Yuan, "Survey on UAV cellular communications: Practical aspects, standardization advancements, regulation, and security challenges," *IEEE Communications Surveys & Tutorials*, vol. 21.4, pp. 3417–3442, March 2019.

[10] A. Al-Hourani, S. Kandeepan, and S. Lardner, "Optimal LAP altitude for maximum coverage," *IEEE Wireless Communications Letters 3.6*, pp. 569–572, Jul 2014.

[11] N. Tafintsev, D. Moltchanov, M. Gerasimenko, M. Gapeyenko, j. Zhu, S.-p. Yeh, N. Himayat, S. Andreev, Y. Koucheryavy, and M. Valkama, "Aerial access and backhaul in mmwave b5g systems: Performance dynamics and optimization," *IEEE Communications Magazine 58.2*, pp. 93–99, Feb 2020.

[12] e. a. Polese, Michele, "Integrated access and backhaul in 5G mmwave networks: Potential and challenges," *IEEE Communications Magazine 58.3*, pp. 62–68, Mar 2020.

[13] C. Pan, J. Yi, C. Yin, J. Yu, and X. Li, "Joint 3D UAV placement and resource allocation in software-defined cellular networks with wireless backhaul," *IEEE Access, 7*, pp. 104 279–104 293, July 2019.

[14] E. Kalantari, M. Z. Shakir, and A. Yongacoglu, "Backhaul-aware robust 3D drone placement in 5G+ wireless networks," pp. 109–114, 05 2017.

[15] E. Kalantari, H. Yanikomeroglu, and A. Yongacoglu, "Wireless networks with cache-enabled and backhaul-limited aerial base stations," *IEEE Transactions on Wireless Communications 19.11*, pp. 7363–7376, July 2020.

[16] A. A. Khuwaja, Y. Zhu, G. Zheng, Y. Chen, and W. Liu, "Performance analysis of hybrid UAV networks for probabilistic content caching," *IEEE Systems Journal*, Aug 17 2020.

[17] T. Zhang, Z. Wang, Y. Liu, W. Xu, and A. Nallanathan, "Caching placement and resource allocation for cache-enabling UAV NOMA networks," *IEEE Transactions on Vehicular Technology, 69.11*, pp. 12 897–12 911, Aug 2020.

[18] ——, "Cache-enabling UAV communications: Network deployment and resource allocation," *IEEE Transactions on Wireless Communications 19.11*, pp. 7470–7483, Jul 2020.

[19] Lazar, R.G, and et al, "Simulated and practical approach to assess the reliability of the 5G communications for the Uu interface," *2022 14th International Conference on Communications (COMM)*, pp. 1–6, June 2022.

[20] Wang, Wei, and et al, "Content delivery analysis in cellular networks with aerial caching and mmwave backhaul," *IEEE Transactions on Vehicular Technology 70.5 (2021)*, pp. 4809–22, Apr 2021.

[21] M. Banagar and H. S. Dhillon, "3d two-hop cellular networks with wireless backhauled uavs: Modeling and fundamentals." *IEEE Transactions on Wireless Communications (2022)*, Feb 2022.

[22] Neetu, R. R, and et al, "Joint bandwidth and position optimization in uav networks deployed for disaster scenarios," *2021 National Conference on Communications (NCC)*, pp. 1–6, July 2021.

[23] A. Fouda, A. S. Ibrahim, I. Guvenc, and M. Ghosh, "UAV-based in-band integrated access and backhaul for 5G communications," *2018 IEEE 88th Vehicular Technology Conference (VTC-Fall)*, pp. 1–5, Aug 2018.

[24] H. Sun, X. Wang, C. Xu, Y. Zhang, and T. QS Quek, "Performance analysis for drone-assisted hetnets with flexible cell association," *ICC 2020-2020 IEEE International Conference on Communications (ICC)*, pp. 1-6 2020.

[25] M. Banagar and H. S. Dhillon, "3D two-hop cellular networks with wireless backhauled UAVs: Modeling and fundamentals," *IEEE Transactions on Wireless Communications*, pp. 6417–6433, Aug 2022.

[26] Zhang, Jing, and et al, "On the application of directional antennas in multi-tier unmanned aerial vehicle networks," *IEEE Access 7 (2019)*, pp. 132 095–132 110, Sep 2019.

[27] Le, N. Phuc, and et al, "Energy-harvesting aided unmanned aerial vehicles for reliable ground user localization and communications under lognormal-nakagami-m fading channels," *IEEE Transactions on Vehicular Technology 70.2 (2021)*, Jan 2021.

[28] I. Atzeni, J. Arnau, and M. Kountouris, "Downlink cellular network analysis with los/nlos propagation and elevated base stations," *IEEE Transactions on Wireless Communications 17.1*, pp. 142–156, Oct 2017.

[29] M. Furqan, Z. Ali, Q. Jan, S. Nazir, S. Iqbal, and Y. Huang, "An efficient load-balancing scheme for uavs in 5g infrastructure," *IEEE Systems Journal (2022)*, 2022.

[30] X. Lin, J. Xia, and Z. Wang, "Probabilistic caching placement in UAV-assisted heterogeneous wireless networks," *Physical Communication 33*, pp. 54–61, 2019.

[31] S. N. Chiu, D. Stoyan, W. S. Kendall, and J. Mecke, *Stochastic geometry and its applications*. John Wiley & Sons, 2013.

[32] W. Yi, Y. Liu, , and A. Nallanathan, "Modeling and analysis of D2D millimeter-wave networks with poisson cluster processes," *IEEE Transactions on Communications*, pp. 5574–5588, Aug 2017.

[33] M. Alzenad and H. Yanikomeroglu, "Coverage and rate analysis for unmanned aerial vehicle base stations with LoS/NLoS propagation," *2018 IEEE Globecom Workshops (GC Wkshps)*, pp. 1–7, 03 2018.

[34] Liu, Yalin, and et al, "Ground-to-uav communication network: Stochastic geometry-based performance analysis," *ICC 2021-IEEE International Conference on Communications*, pp. 1–6, 6 2021.

Anand Srivastava did his M.Tech. and Ph.D. from IIT Delhi and is currently working at IIIT Delhi as a Professor in ECE department since Nov. 2014 and also Director at IIIT Delhi Incubation Center (a Section 8 company). He is also Adjunct faculty in Bharti School of Telecom Technology at IIT Delhi. He was Dean & Professor in the School of Computing and Electrical Engineering at Indian Institute of Technology Mandi, HP, India for 2 years. In his initial stint of 20 years, he was with the Center for Development of Telematics (CDOT), a telecom research center of Govt. of India where he was Director and member of the CDOT Board. Currently, he is driving VLC/LiFi standardization activities under the aegis of TSDSI. His research work is in the area of optical core & access networks, Vehicle-to-vehicle communications, Fiber-Wireless (FiWi) architectures, and Visible light communications.

Neetu R.R received her BTech and Mtech in communication engineering and signal processing from the University of Calicut, India. Currently, she is pursuing her Ph.D. from Indraprastha Institute of Information Technology (IIIT), Delhi. During her MTech, she worked as a Research Assistant in the Defence Research and Development Organization (DRDO), Bangalore, India. Her research interests are stochastic geometry for heterogeneous networks (HetNets) and wireless communications

Vivek Ashok Bohara a (Senior Member, IEEE) received his Ph.D. degree from Nanyang Technological University, Singapore, in 2011. From 2011 to 2013, he was a Postdoctoral Researcher (Marie Curie fellowship), ESIEE Paris, University Paris-East, Créteil, France. In 2013, he joined Indraprastha Institute of Information Technology-Delhi, India, where he is currently Head and Professor (ECE). He has authored and co-authored more than 50 publications in major IEEE/IET journals, refereed international conferences, two book chapters, and one patent. His research interests include next-generation communication technologies, such as device-to-device communication, carrier aggregation, and visible light communications. Dr. Bohara was the recipient of the First Prize in National Instruments ASEAN Virtual Instrumentation Applications Contest in 2007 and 2010, Best Poster Award at the IEEE ANTS 2014 and the IEEE Comsnets 2015 and 2016 conferences.

Gourab Ghatak received his Ph.D. from Telecom ParisTech (University of Paris Saclay), France, during which he was also employed in CEA Grenoble, France. Currently, he is an Assistant Professor at the Department of Electrical Engineering at the Indian Institute of Technology Delhi (IIT Delhi). His research interests are stochastic geometry and machine learning for wireless communications.